Metformin Confers Cardiac and Renal Protection in Sudden Cardiac Arrest via AMPK Activation

Cody A. Rutledge MD, PhD[1], Claudia Lagranha PhD[1], Takuto Chiba PhD[2,3], Kevin Redding MS[1], Donna B. Stolz PhD[4], Sunder Sims-Lucas PhD[2,3], Cameron Dezfulian MD[5], Jonathan Elmer MD, MS[6], Brett A. Kaufman PhD[1]

1. Division of Cardiology, Vascular Medicine Institute, Department of Medicine, University of Pittsburgh, Pittsburgh, PA, USA

2. Rangos Research Center, Children's Hospital of Pittsburgh, University of Pittsburgh, Pittsburgh, PA, USA

3. Division of Nephrology, Department of Pediatrics, University of Pittsburgh School, Pittsburgh, PA, USA

4. Department of Cell Biology, University of Pittsburgh, Pittsburgh, PA, USA

5. Department of Critical Care, Texas Children's Hospital, Houston, TX, USA

6. Departments of Emergency Medicine, Critical Care Medicine, and Neurology, University of Pittsburgh, Pittsburgh, PA, USA

Corresponding Author:

Brett A. Kaufman

200 Lothrop Street

BST E1241

Pittsburgh, PA 15261

1-412-624-8644

bkauf@pitt.edu

Conflicts of Interest and Source of Funding:

The authors of this manuscript have no financial or ethical conflicts of interest to disclose.

Abstract

Sudden cardiac arrest (SCA) affects over 600,000 individuals annually in the United States and is associated with substantial mortality. After resuscitation, multi-system organ damage is common and largely attributable to ischemia-reperfusion injury. The anti-diabetic drug metformin improves cardiac outcomes in models of myocardial ischemia and ischemia-reperfusion. In this study, we evaluated the role of metformin pretreatment in a mouse model of SCA. We found that two weeks of metformin pretreatment protects cardiac ejection fraction and reduces acute kidney injury post-SCA in non-diabetic mice. Further, metformin pretreatment prior to SCA activates AMPK signaling and is associated with altered mitochondrial dynamics and markers of autophagy following arrest. Direct AMPK activation and inhibition studies demonstrate that activation is necessary and sufficient for metformin-mediated protection of cardiac and renal tissues in this model. We were unable to demonstrate cardiac protection with a single-dose metformin rescue therapy. Importantly, these findings translate into patients. We retrospectively evaluated the extent of cardiac and kidney damage in diabetic patients resuscitated from SCA. Metformin-treated patients have less evidence of heart and kidney damage after arrest than diabetics who have not received metformin. Together, these data support AMPK activation as a preventive mechanism in ischemia-reperfusion injury.

Introduction

Sudden cardiac arrest (SCA) refers to the abrupt cessation of cardiac function and affects over 600,000 patients annually in the United States (1,2). Patients with return of spontaneous circulation after SCA experience systemic ischemia-reperfusion injury, typically resulting in multi system organ damage. Common findings include cardiogenic shock, acute renal failure, liver damage, and neurologic dysfunction (3–5). Previous observational studies in cardiac arrest patients have shown that low cardiac ejection fraction (EF) (6) and reduced kidney function (7,8) are predictors of increased mortality. Despite its prevalence, no pharmacologic therapy has been shown to improve overall survival in post-cardiac arrest syndrome.

Metformin is an oral antihyperglycemic agent used as the first-line agent for type 2 diabetes that has proven beneficial in a number of cardiovascular conditions(9,10). Metformin enhances insulin sensitivity and normalizes glucose and lipid homeostasis (11–13). Beyond its role in controlling diabetes, metformin has demonstrated clinical benefit across a wide variety of pathologies, including improved mortality in the setting of coronary artery disease (10), congestive heart failure (14), acute kidney injury (AKI)(15), chronic kidney disease (14), septic shock (16,17), and major surgical procedures (18). Cardiovascular studies suggest that improved outcomes occur independently of the glucose-lowering effects of metformin and may instead be attributable to metformin's other pleiotropic effects (19). Several mechanisms beneficial to cardiovascular health have been implicated in metformin's numerous effects, including reduced oxidative stress, anti-apoptotic activities, JNK inhibition, complex I inhibition, and AMPK activation (20,21).

Importantly, AMPK activity and expression is induced in mice and humans by ischemic stress as a compensatory response (22). AMPK activity limits endoplasmic reticulum (ER) stress (23) and AMPK deficiency can be partially rescued through reduction of mitochondrial oxidative stress (24). While AMPK activity is essential for survival after ischemic stress (23), it is unclear whether AMPK activity is the mediator of metformin-mediated protection in ischemic heart disease. Furthermore, it is not clear whether the adaptive upregulation of AMPK during cardiac stress is optimal, or whether further activation could even more strongly impact recovery in cardiac injury models.

In this study, we sought to test metformin's potential benefit on heart and kidney protection after SCA, both to clarify its relevance to the development of cardiac and peripheral tissue dysfunction, and to determine the role of AMPK in post-arrest outcomes. Therefore, we evaluated outcomes following SCA in mice with chemical activation of AMPK, via 5-aminoimidazole-4-carboxamide-1-β-D-ribofuranoside (AICAR; an AMP-mimetic(25)) and with metformin treatment, and with inhibition of AMPK via compound C (a reversible competitive inhibitor(26)) given concomitantly with metformin treatment. We found that both metformin and AICAR pretreatment improved cardiac and renal outcomes after resuscitation from SCA, and that metformin therapy is associated with altered markers of autophagy and mitochondrial dynamics. We also showed that metformin's benefits are negated by compound C, supporting an AMPK-dependent mechanism. Further, we performed a retrospective analysis of clinical outcomes in diabetic cardiac arrest patients with and without metformin therapy prior to arrest. We found that diabetic patients taking metformin prior to SCA had lower serum markers of cardiac and renal damage 24 hours after arrest than non-metformin diabetic patients. Taken together, we have identified AMPK activity as a protective mechanism invoked SCA-induced damage and

demonstrated benefit of metformin pretreatment on cardiac and renal outcomes in SCA, which provides substantial support for metformin's use as a prophylactic in patients at risk for SCA.

Results

SCA mice have increased AMPK signaling by pathway analysis

To gain insight into gene expression pathways affected in the heart *in vivo* after SCA, we performed microarray analysis of left ventricles (LVs) 24 hours post-resuscitation. In these initial discovery experiments, male and female mice were evenly divided into untreated sham and untreated arrest groups, where the arrest group underwent ultrasound-guided direct LV injection of potassium chloride (KCl) to cause SCA (Figure 1A). In brief, these mice sustained eight minutes of asystole followed by up to three minutes of cardiopulmonary resuscitation (CPR) until return of spontaneous circulation (ROSC) occurred. One day after surgery, LV tissue was collected for RNA expression analysis (Figure 1B). From Ingenuity Pathway Analysis, *AMPK Signaling* pathway was the most prominent by ranked p-value, while *Autophagy* was the sixth most significantly changed pathway between sham and untreated SCA mice (Figure 1C, Supplemental Figure 1).

Metformin pretreatment protects cardiac EF and kidney function after SCA

AMPK signaling has been shown to be upregulated in myocardial ischemia/reperfusion injury as a compensatory response (27). Similarly, loss of key AMPK subunits increases infarct size in experimental systems (23,24). In *ex vivo* rat hearts, infarct size can be reduced by acute, transitory AMPK activation (28,29). Furthermore, AMPK activation has been shown to delay the progression of heart failure in a chronic pressure overload model (30). Although the etiology of cardiac dysfunction in myocardial infarction and pressure overload is distinct from SCA, we reasoned that further enhancing AMPK activity could show functional cardiac benefits in the *in vivo* SCA model. To test this hypothesis, male and female mice were divided into sham and arrest groups, with and without metformin pretreatment. Metformin-treated mice were given 1 mg/mL of metformin in water for two weeks. There were no significant differences among baseline animal characteristics, including weight, ratio of female mice, or EF (Table 1, Figure 2A). Importantly, there were no differences among groups for body weight in these non-diabetic mice. Twenty-four hours after surgery, untreated arrest mice had significantly lower EF than untreated sham mice (sham: 59.5±1.7%; untreated arrest: 41.1±2.7%, $p<0.0001$, Figure 2A), as expected based on our previous description of this model(31). Importantly, metformin pretreatment significantly improved EF 24 hours post-SCA (arrest metformin: 51.6±2.6%, $p<0.01$ vs. untreated arrest) to a level not significantly different from sham mice (Figure 2A). There were no changes to post-operative body temperature, time to resuscitation, or 24-hour glucose levels between arrest groups (Table 1). The lack of detectable changes in body weight or in the 24 hour post-SCA glucose suggests that differences in systematic glucose handling was inadequate to explain later phenotypes.

The effects of whole-body ischemia/reperfusion injury can be detected in peripheral tissues, particularly in the kidney (31). Unsurprisingly, untreated arrest mice had significant kidney damage when compared to untreated sham mice at one day post-SCA. Kidney damage was quantified by serum creatinine (sham: 0.36±0.04 mg/dL; untreated arrest: 1.49±0.14 mg/dL, $p<0.0001$, Figure 2B-C) and blood urea nitrogen (BUN) levels (sham: 26.6±5.2 mg/dL; untreated arrest: 153.9±28.4 mg/dL, $p<0.001$), and tubular injury score by histological analysis (sham: 0.11±0.04; untreated arrest: 3.33±0.24, $p<0.0001$). The 1 mg/mL metformin-pretreated arrest mice had some improvement over untreated arrest mice, with significantly reduced creatinine levels (metformin arrest: 0.92±0.24 mg/dL, $p<0.05$ vs. untreated arrest). However, metformin treatment did not fully protect kidneys from SCA-induced damage because serum creatinine was still significantly elevated compared to untreated sham ($p<0.05$

vs. sham), as was BUN (121.2±28.0 mg/dL, p<0.05 vs. sham). Similarly, histological analysis revealed an increase in tubular injury score in metformin arrest mice (2.26±0.24, p<0.0001 vs. sham) that was partially improved compared to untreated arrest (p<0.01; Figure 2B-C). Metformin pretreatment in sham mice did not significantly affect creatinine levels (0.38±0.06 mg/dL), BUN (28.8±9.4 mg/dL), or tubular injury score (0.14±0.04; Figure 1C) relative to untreated sham. The time of renal ischemia was unchanged between untreated and metformin-pretreated arrest groups (Figure 2D; Table 1), suggesting the reperfusion differences were not a component of kidney protection.

Metformin dosage has been a concern for patients with preexisting kidney damage, especially for those with chronic kidney disease, but lower doses have been found safe and avoid hyperlactatemia (32,33). Furthermore, data have suggested that differences in dosage alter metformin targets, with low doses activating AMPK, but higher doses causing mitochondrial Complex I inhibition(34). We therefore treated an additional mouse cohort with a lower dose of metformin (0.2 mg/mL in drinking water as opposed to 1 mg/mL in Figure 2) to reduce potential complications of decreased metformin clearance after arrest. We found that the low-dose metformin cohort did not have significant cardio-protection when compared to untreated arrest mice (EF of low-dose metformin: 50.7±3.3%, p=0.08 vs. untreated arrest) (Supplemental Figure 3A), though this cohort may not have been powered to detect cardiac changes. However, the low-dose metformin arrest cohort did have lower serum creatinine (0.40±0.05 mg/dL, p<0.001 vs. untreated arrest) and BUN levels (64.83±8.24 mg/dL, p<0.05 vs. untreated arrest), but unchanged tubular injury when compared to untreated arrest mice (2.04±0.71, p=0.08 vs. untreated arrest) (Supplemental Figure 3). These results suggest superior protection against kidney damage with low-dose metformin over the higher dose metformin pretreatment, and protection against ischemia/reperfusion injury by metformin need not be through mitochondrial respiration dysfunction.

Metformin promotes AMPK activation in the LV following SCA

As a marker of total AMPK activation, we assessed phosphorylation of threonine-172 of the AMPKα subunit (35). One day after surgery, LVs from sham and arrest groups with and without metformin pretreatment (n=6/group) were assessed for p-AMPK, total AMPK, and glyceraldehyde 3-phosphate dehydrogenase (GAPDH) protein expression (Figure 2E). Surprisingly, metformin treatment did not appear to cause activation of p-AMPK/AMPK in the sham mice (untreated sham: 1.00±0.13; metformin sham: 0.80±0.11). However, we found significantly elevated p-AMPK/AMPK in metformin-pretreated arrest mice (1.52±0.14 AU) when compared to untreated sham (1.00±0.13 AU, p<0.05), untreated arrest (0.70±0.12, p<0.001), and metformin-pretreated sham mice (0.80±0.11, p<0.01). p-AMPK/GAPDH was similarly elevated in the LVs of metformin arrest mice (1.47±0.08 AU) when compared to untreated sham (1.00±0.10 AU, p<0.05), untreated arrest (0.90±0.14 AU, p<0.01), and metformin-pretreated sham (0.98±0.09 AU, p<0.05). Total AMPK/GAPDH was not significantly changed between groups. These data suggest that cardiac injury with metformin-pretreatment increases the potential for AMPK activation.

AMPK activation causes cardiac and renal protection after SCA and is necessary for metformin's protection of EF

Because metformin has multiple potential modes of action, we tested whether direct AMPK activation was sufficient for the observed enhanced EF, and whether metformin benefit in SCA depended on AMPK activity. To that end, male and female mice were divided into two groups: 1) AICAR

pretreatment, which activates AMPK (36), and 2) metformin-pretreatment combined with compound C, an established AMPK inhibitor (13). Both groups underwent two weeks of intraperitoneal (IP) injections prior to SCA and subsequent evaluation 24-hours after arrest. These groups were compared to the untreated arrest and metformin pretreated arrest mouse results described above. One day after surgery, AICAR pretreated arrest mice had significantly improved EF when compared untreated arrest mice (AICAR arrest: 52.0±2.4%, $p<0.05$ vs. untreated arrest, Figure 3A). Compound C not only prevented the beneficial effects of metformin on post-SCA EF, but also caused significantly reduced EF (metformin + C arrest: 30.0±2.9%) when compared to untreated arrest ($p<0.05$). There was no change to body weight, ratio of female mice, or baseline EF (Table 1 and Supplemental Figure 2) prior to arrest. The effects of AICAR pretreatment phenocopies metformin pretreatment, and compound C blocks the benefit of metformin strongly suggest that AMPK activation is necessary and sufficient for the metformin-mediated protection of cardiac function after SCA. We cannot rule out the involvement of involvement of glucose homeostasis and insulin sensitivity as contributing factors in this process. We have not observed differences in random glucose and insulin levels, suggesting that such an effect would be modest.

In the same cohort of mice, measures of kidney damage were significantly lower in AICAR-pretreated mice than untreated arrest mice. Both creatinine (AICAR arrest: 0.67±0.25 mg/dL, $p<0.05$, Supplemental Figure 4A) and tubular injury score (AICAR arrest: 1.45±0.42, $p<0.01$) were significantly improved relative to untreated arrest mice (creatinine 1.49±0.14 mg/dL, tubular injury score 3.33±0.24). In contrast, there was no significant change when comparing renal outcomes in metformin-treated and metformin + compound C-treated arrest mice (Supplemental Figure 4A). AICAR phenocopied the metformin benefit in measures of kidney function and damage, suggesting a role for AMPK activation in those processes. The limited change in these measures in the metformin + compound C cohort vs. untreated arrest mice may suggest that at baseline AMPK activation is limited and cannot be further reduced but would require further experimentation.

AICAR promotes AMPK activation in the LV following SCA

Twenty-four hours after surgery, LVs from arrest groups (n=6) were assessed for AMPK and p-AMPK expression (Figure 3B). As expected, p-AMPK/AMPK was significantly elevated in AICAR-pretreated arrest mice (AICAR arrest: 2.54±0.59 AU) when compared to untreated arrest (1.00±0.17 AU, $p<0.05$). p-AMPK/GAPDH and AMPK/GAPDH were not significantly changed in the AICAR group. Metformin + compound C pretreated mice had lower p-AMPK/AMPK than the AICAR group (arrest metformin + C: 0.52±0.13 AU, $p<0.05$) and p-AMPK/GAPDH (0.54±0.11 AU, $p<0.05$) but no significant change from the untreated arrest group.

Metformin affects mitochondrial morphology and markers of mitochondrial dynamics and autophagy

Since ischemia/reperfusion is well known to induce mitochondrial damage, electron microscopy was used to identify differences in mitochondrial perimeter, area, and circularity among in hearts of untreated sham, untreated arrest, and metformin-pretreated arrest mice (Figure 4A). The untreated arrest mice showed a decrease in mitochondrial perimeter and area (perimeter: 3.06±0.06 μm; area: 0.60±0.02 μm^2; Figure 4B) when compared to sham (perimeter: 3.81±0.09 μm; area: 0.87±0.04 μm^2, $p<0.0001$ for both measures). Metformin-pretreated arrest mice showed a modest but significant increase of perimeter and area (perimeter: 3.33±0.07 μm; area: 0.70±0.03 μm^2) when compared to untreated arrest mice ($p<0.05$ for both measures). Both the untreated arrest mice (0.76±0.001 μm,

p<0.0001) and metformin-pretreated arrest mice (0.75±0.01 µm; p<0.0001) had more circular mitochondria than the untreated sham mouse mitochondria (0.69±0.01 µm). These data demonstrate changes in mitochondrial morphology at 24 hours post-SCA, with improvements in mitochondrial area and perimeter in metformin-pretreated arrest mice compared to untreated arrest mice.

We also looked at markers of mitochondrial abundance in the LVs. First, representative proteins of mitochondrial respiratory complexes were assessed from LV extracts taken 24 hours after arrest from untreated sham, untreated arrest, metformin-pretreated sham, and metformin-pretreated arrest mice. There was a mild but significant elevation in relative complex II expression in the metformin-pretreated arrest mice (1.29±0.10 AU) compared to untreated sham mice (0.98±0.04 AU, p<0.01), but otherwise, relative expression of representative proteins was unchanged across the groups (Figure 4C). Second, we examined mtDNA relative abundance and damage in the cardiac tissue from these groups. Unlike in failed hearts (37), the arrest group did not show a statistically significant decrease in mtDNA levels at 24 hours post-SCA. The metformin-pretreated arrest mice had slightly higher relative mitochondrial DNA (mtDNA) levels (1.16±0.06 AU) than untreated arrest mice (0.89±0.05 AU, p<0.05, Figure 4D), but were not significantly different from the sham group (1.00±0.05 AU). Interestingly, the metformin-pretreated arrest mice had significantly less mtDNA damage (0.03±0.1 lesions/10kb mtDNA) than untreated arrest mice (0.59±0.16 lesions, p<0.05) as measured by long extension PCR assays. The small but significant increases in mtDNA and complex II in the metformin-pretreated arrest mice are consistent with an increase in mitochondrial biogenesis, but the significant improvement in mtDNA integrity suggests an improvement in overall mitochondrial quality.

To better understand the alterations in mitochondrial morphology, we examined the relative levels of several proteins involved in establishing mitochondrial shape. Mitofusin 2 (MFN2), a mitochondrial outer membrane GTPase involved in fusion, had reduced expression in metformin-pretreated arrest mice (0.53±0.07 AU) compared to all other groups (sham: 1.00±0.10 AU, p<0.01; arrest: 1.06±0.07 AU, p<0.001; sham metformin: 0.89±0.04 AU, p<0.05; Figure 5A). OPA1, also a dynamin-related GTPase, resides in the inner membrane to perform fusogenic functions(38), and followed a similar overall trend with significantly reduced levels in metformin-pretreated arrest mice (0.75±0.04 AU) when compared to untreated arrest mice (1.13±0.10 AU, p<0.05). In contrast, dynamin-related protein 1 (DRP1), whose activity is regulated by its phosphorylation at Ser-616(39), showed no significant change in p-DRP/DRP between sham and arrest groups. Metformin pretreatment appeared to modestly improve p-DRP/DRP post-arrest but the effect was not statistically significant (p=0.08). While mitochondrial perimeter and area are increasing with metformin-pretreatment in SCA hearts, markers of fusion decrease and fission is unchanged from sham or arrest. The MFN2 decrease may instead suggest that other mitochondrial quality control processes contribute to the improved mitochondrial morphology.

Interestingly, MFN2 decrease is consistent with the activation of mitophagy (40,41), due to its ubiquitination and targeted proteolysis during autophagy. Metformin has been reported to impact heart autophagy through AMPK signaling (42,43). To test engagement of autophagy in the SCA model, LVs collected 24 hours after SCA from untreated sham, untreated arrest, metformin-pretreated sham, and metformin-pretreated arrest mice were evaluated for markers of autophagy by western blot analysis. First, we evaluated the mTOR signaling pathway, a crucial negative regulator of autophagy (44). Consistent with prior findings (45), we found the marker of mTOR activity, p-mTOR (Ser-2448), to be significantly reduced in untreated arrest (0.58±0.08 AU, p<0.05), metformin-pretreated sham (0.55±0.08

AU, p<0.05), and metformin-pretreated arrest mice (0.53±0.07 AU, p<0.05) when compared to sham mice (1.0±0.15 AU, Figure 5A). Total mTOR protein (mTOR/GAPDH) was only reduced in the metformin-pretreated arrest group (0.71±0.08 AU) when compared to sham (1.00±0.05 AU, p<0.05) and untreated arrest (0.96±0.06 AU, p<0.05) groups. The ratio of p-mTOR to total mTOR was unchanged between groups, but we focus on p-mTOR/GAPDH as a measure of activity. As positive downstream markers of mTOR activity, S6 ribosomal protein (S6) total expression and phosphorylation at Ser-240/244 (p-S6) were assessed. We found that p-S6 (pS6/GAPDH) was reduced in untreated arrest (0.41±0.05 AU, p<0.01) and metformin-pretreated arrest mice (0.52±0.07 AU, p<0.05) when compared to sham (1.00±0.17 AU; Figure 5B). Total S6 was increased in the metformin sham mice compared to untreated sham (1.40±0.08 AU, p<0.05) and decreased in metformin-pretreated arrest mice (0.80±0.05 AU, p<0.001) when compared to untreated sham mice (1.00±0.10 AU). p-S6/S6 was significantly reduced in the untreated arrest mice (0.49±0.08 AU) when compared to untreated sham mice (1.00±0.17 AU, p<0.05). p-S6 levels are increased with metformin in sham mice, consistent with the metformin activation of mTOR observed in other contexts (43). However, because mTOR activity based on p-mTOR and pS6 are not significantly different between arrest and metformin arrest mice, the data suggest that decreased mTOR activation alone is insufficient to explain the survival benefit of metformin.

Because metformin has been reported to increase cardiac mitophagy in cardiomyopathy (42,43), we evaluated protein expression for markers associated with autophagosome formation, including p62/Sequestosome 1, a cargo receptor associated with degradation of ubiquinated proteins (46), and LC3 processing. p62 expression (normalized to GAPDH) was significantly lower in the metformin arrest mice (0.67±0.09 AU) when compared to the untreated arrest group (1.22±0.10 AU, p<0.05, Figure 5B). The relative levels of microtubule-associated protein light chain 3 (LC3), specifically levels of uncleaved (LC3-I) and cleaved (LC3-II) forms, were also monitored as an indicator of changes in autophagy initiation(47). Interestingly, the LC3-II to LC3-I ratio was significantly increased in untreated arrest mice (1.91±0.15 AU) compared to sham (1.00±0.18 AU, p<0.01), whereas the metformin-pretreated arrest mice had significantly reduced LC3-II/LC3-I (1.17±0.17 AU) when compared to untreated arrest mice (p<0.05, Figure 5B). LC3-I and LC3-II expression levels (normalized to GAPDH) were not significantly changed between groups (Supplemental Figure 5). The restoration of p62 and LC3-II/I to untreated sham levels in metformin-pretreated LVs after SCA appears to associate with the improvements in the mitochondrial area and perimeter in the metformin arrest hearts vs. the sham arrest hearts.

Taken together, these data suggest that increase autophagic flux contributes to the improved mitochondrial network in metformin-pretreated arrest mice. Metformin increases the mitochondrial perimeter and area despite the decrease in MFN2 and OPA1 fusogenic proteins. Further, there is an increase in p62 and LC3-II in arrest hearts, which is consistent with impaired autophagic flux observed by others(48). Notably, metformin pretreatment reduced p62 and LC3-II levels and significantly improved mtDNA integrity after SCA, suggesting that autophagy in those hearts was also improved, which is consistent with the observed lower level of mitochondrial fragmentation. Additional studies are required to analyze flux in real-time.

Metformin does not improve outcomes as a rescue therapy

In *ex vivo* studies of ischemia-reperfusion, acute metformin administration just prior to stop-flow mediated injury improved developed pressures during recovery(44). In ligation-mediated

ischemia/reperfusion experiments *in vivo*, 125 µg/kg metformin injection into the LV lumen at the time of reperfusion resulted in a decreased infarct area and improved EF in non-diabetic mice(45). In contrast to coronary artery ligation experiments, which generally rely on >30 minute ischemic times and generate significant cardiomyocyte death, our SCA model is 8 minutes of ischemia and lacks overt cell death(29). In our SCA model, when metformin was given directly into the LV at resuscitation as a rescue therapy (1,250 µg/kg), there was no change to EF at one day after SCA (arrest rescue metformin: 42.1±2.4%) compared to untreated arrest mice (Figure 6). Similarly, there was no change in creatinine (arrest rescue metformin: 1.2±0.25), BUN (arrest rescue metformin: 155.3±14.2), or tubular injury score (arrest rescue metformin: 2.45±0.55) when compared to untreated arrest mice (Supplemental Figure 4B). Baseline EF was not significantly different between groups (Supplemental Figure 2). These data are consistent with the notion that metabolic adaptation is required for the metformin protection after SCA.

Metformin improves markers of cardiac and renal damage in humans one day after SCA

Data supporting metformin use in cardiovascular disease are conflicting, often varying with the particular condition or disease (21). To mirror our observations in mice, we focused in this retrospective study on diabetic patients who survived to hospital care after resuscitation from SCA. Some of these patients were taking metformin prior to SCA. We started with clinical data from 2,692 patients treated at a single academic medical center, of whom 692 (26%) had a history of diabetes. We excluded 268 patients with chronic kidney disease, 20 who were transferred to our facility more than 24 hours post-arrest, 56 for whom home medications were unknown, 7 who rearrested prior to labs being drawn, and 1 who was resuscitated with extracorporeal membrane oxygenation, leaving 341 patients in our final analysis. Mean age was 65 ± 13 years, and 148 (43%) were female (Table 2). Overall, 140 (41%) patients were prescribed metformin prior to arrest, 153 (45%) were prescribed insulin, and 92 (27%) were prescribed other oral hyperglycemic medications. Serum troponin and creatinine were measured as part of routine clinical care, typically at least once daily, and used to quantify heart and kidney injury, respectively. We did not find reliable echocardiography data in this cohort. Median peak troponin in the first 24 hours post-arrest was 1.4 (interquartile range, IQR: 1.0-1.7) and median peak creatinine was 1.4 (IQR: 1.0-2.0). We used generalized linear models (gamma distribution, log link) to test the independent association of pre-arrest metformin use with peak troponin and creatinine within 24 hours after SCA, adjusting for clinically relevant confounders including age, sex, arrest location (in- vs out-of-hospital), witnessed collapse, layperson CPR, number of epinephrine doses administered, cardiac etiology of arrest, and Charlson comorbidity index, as well as the use of insulin or other oral hyperglycemic medications (Table 2). We handled the 2% missing data using multiple imputations. Metformin prescription at the time of SCA was independently associated with lower 24-hour peak serum troponin and lower 24-hour peak serum creatinine (Table 3). Without A1C levels, we cannot rule out whether there are differences in glycemic control that associate with the improved cardiac and renal measures in these patients.

Discussion

SCA is a common cardiac event for which there are extremely poor outcomes and no current course-altering interventions. Metformin therapy, a first-line diabetes treatment, is beneficial in a number of cardiovascular disorders(9,10)making it a candidate approach for SCA. Metformin impacts many metabolic processes, including activation of the AMPK signaling pathway, decreased ER stress and ROS, improved autophagy and mitochondrial biogenesis, and inhibition of the mitochondrial permeability transport pore (mPTP) (49–53). Studies of metformin's effects on cardiac function have largely utilized ischemia-reperfusion injury models with ischemic periods of 25-30 minutes, both *in vivo* and *ex vivo*. Metformin, applied as a therapy, decreases scar size in reversible coronary artery ligation (21,28,53–56) or whole-heart ischemia-reperfusion (21,57), respectively. The long ischemic duration in these models involves substantial cardiomyocyte necrosis, and much of metformin's beneficial effect has been attributed to reduction of mPTP-mediated cell death in the infarct border zone (49). In contrast, our data demonstrates metformin's protection of *in vivo* EF in a SCA model that features 8 minute ischemia period without evidence of cardiac cell death (31). Therefore, with a shorter ischemic duration and no evidence of apoptosis, we have identified a unique pathway of metformin's cardiac protection.

The requirement of AMPK signaling for metformin's cardiac benefits was confirmed by downstream inhibition and rescue experiments. Specifically, metformin's effects were negated by concomitant treatment with the AMPK inhibitor compound C and were replicated by treatment with the direct AMPK activator AICAR alone. Taken together, these data rigorously support that AMPK activation is sufficient and necessary for cardiac protection.

Metformin pretreatment also protects against kidney injury in our model of SCA, reducing creatinine levels, BUN, and tubular injury scores (Figure 2). As there is no change to ischemic duration in the kidneys between untreated arrest and metformin-pretreated arrest mice, as measured by renal artery doppler ultrasound (Table 1), this renal protection is likely intrinsic to the kidney rather than secondary to the improved cardiac function. Previous studies have demonstrated beneficial effects of metformin on renal performance after primary renal ischemic injury (58–60). Our model extends the known impact of metformin on renal function by demonstrating comparable beneficial effects in a model featuring renal ischemia secondary to cardiac arrest, more analogous to clinically observed renal injury.

There exists concern about metformin therapy in the presence of kidney injury, as metformin accumulation can lead to potentially lethal lactic acidosis (33). While we did not assess lactate build-up or metformin accumulation in our model, we did treat an additional cohort of mice with a lower dose of metformin (Supplemental Figure 3), comparable to concentrations of human doses, to address concerns about supra-pharmacologic metformin concentrations (61). We found that low-dose metformin conferred better renal protection than standard-dose metformin, as measured by creatinine levels after arrest (Supplemental Figure 3B), though cardiac EF improvement did not reach significance in this group. There has been some concern about the mechanism of action in high-dose vs. low-dose metformin therapy; recent work has demonstrated that supra-pharmacologic doses of metformin effect change through inhibition of mitochondrial ATP production, whereas pharmacological doses of metformin increase mitochondrial respiration and fission (62). The literature would suggest that our high-dose metformin (1 mg/mL) is a Complex I inhibitor, whereas low-dose metformin (0.2 mg/mL) activates

AMPK. Our work did not confirm or explore the mechanistic differences between these two doses, which would be a natural extension of this work in the SCA mouse model.

Metformin therapy has pleiotropic effects and a large number of molecular pathways are implicated in metformin's physiological effects, including reducing oxidative stress, inhibiting apoptosis, complex I inhibition, and AMPK activation (19,21,34,63). Pathway analysis of microarray data from SCA mice hearts compared to sham mice implicated AMPK signaling as the most significantly changed pathway in our model (Figure 1C). The rescue of cardiac dysfunction by metformin and AICAR suggests that additional AMPK activation is both possible and beneficial. Reciprocally, mice that were concomitantly treated with metformin and the AMPK inhibitor compound C had significantly lower EF than untreated arrest mice (Figure 3A). Unexpectedly, metformin + compound C mice had lower serum creatinine than the arrest mice, though these studies will need to be confirmed in larger cohorts (Supplemental Figure 4A). Despite this paradox, these data demonstrate that AMPK activation alone is sufficient to cause at least cardioprotection in our SCA model, and that metformin's cardioprotective benefits are negated by AMPK inhibition.

The downstream mechanisms underlying metformin's benefits in our model are difficult to fully elucidate, as both metformin and AMPK signaling have been implicated in a wide number of signaling cascades (21,27,64). However, we observed that the mitochondria in LVs of SCA mice are smaller and rounder than sham cohorts by electron microscopy, and that metformin-pretreated arrest mice have significantly larger mitochondria then untreated arrest mice (Figure 4), which suggest a possible role for alterations in either mitochondrial dynamics or mitophagy as regulators of mitochondrial morphology. Electron transport chain complex abundance estimates were largely unchanged between treatment groups, except for a mild elevation in complex II expression in the metformin-pretreated arrest mice over the sham cohort (Figure 4B). mtDNA copy number and damage were not significantly elevated in the untreated arrest mice when compared to sham, but metformin pretreatment did drive an increase in mtDNA copy number and a decrease in mtDNA damage when compared to the untreated arrest mice (Figure 4D). These data could support an increase in mitochondrial biogenesis or a change in mitochondrial turnover.

There were notable changes to markers of autophagy and mitochondrial dynamics, both of which have been implicated as altered pathways related to AMPK signaling (64–67). We found evidence of decreased expression levels of p-mTOR and p-S6 in untreated arrest, metformin sham, and metformin arrest groups when compared to sham mice as indicated (Figure 5B), which could indicate increased autophagic poise in the case of sham metformin hearts, and either poise or activation of autophagy in the arrest and metformin-pretreated arrest samples. Importantly, an increase in LC3-II/LC3-I occurred in arrest samples but was completely restored to baseline in metformin-pretreated arrest samples. P62, another marker of the autophagosome, was not significantly changed in the untreated arrest vs sham samples but was reduced in metformin-pretreated arrest mice compared to untreated arrest (Figure 5B). These findings are consistent with an increase in autophagy with arrest, which was improved by either decreased mtDNA damage or increase autophagic clearance in the metformin arrest hearts. Because mtDNA damage levels increased in metformin-pretreated arrest hearts beyond control levels, the data suggest increased clearance of damaged mitochondria. SCA causes increased relative fission to untreated sham in heart, but metformin, which improves mitochondrial morphology, does not increase markers of fusion such as p-DRP1. It is unlikely that metformin pretreatment restores fusion, as MFN2 and OPA1 are both further depleted in metformin arrest mice relative to the arrest mice. Importantly,

419 depletion of MFN2 and OPA1 is associated with the induction of autophagy (68), suggesting that
420 clearance is enhanced in the metformin-treated SCA mice. Although this study lacks directed measures
421 of mitochondrial flux, the data are consistent with that metformin pretreatment decreased proteotoxic
422 stress in hearts and more efficient turnover of mitochondria and removal of damaged mtDNA, which
423 increase the overall quality of the mitochondria at 24 hours post-arrest.

424 While metformin pretreatment has been shown to be cardioprotective, it is thus far not a
425 clinically relevant model of therapeutic (post-arrest) intervention for SCA. There exists controversy
426 about the benefits of acute metformin therapy in cardiac ischemia and metformin's role as a rescue
427 therapy. Mouse studies of ischemia-reperfusion have demonstrated reduced infarct size when treated
428 with metformin at the time of coronary artery ligation(52) or after ischemic insult(69). However, these
429 benefits were not shown in a swine model of coronary artery ligation treated with metformin at the
430 time of reperfusion(70). We attempted to treat our SCA mice with acute metformin via left-ventricular
431 injection given at the time of reperfusion but found no evidence of cardiac (Figure 6) or renal
432 (Supplemental Figure 4B) protection in this model (Figure 6). Our data do not prove, but are supportive
433 of the idea, that metabolic adaptation is necessary to convey protection in a preventative setting.

434 To evaluate the clinical relevance of the cardiac and renal protection demonstrated with
435 metformin pretreatment in our SCA mouse model, we performed a retrospective analysis of diabetic
436 patients resuscitated from cardiac arrest. We divided these patients into metformin-treated and non-
437 metformin-treated patients. Our primary endpoints were peak serum troponin within 24 hours post-
438 arrest as a marker of cardiac damage and peak serum creatinine within the first 24 hours as a marker of
439 kidney damage. Multiple regression analyses demonstrated a significant association between metformin
440 pretreatment and decreased peak serum troponin and peak serum creatinine levels (Table 3). This
441 suggests that metformin is driving cardiac and renal protection independently of other baseline
442 characteristics. Previous studies have noted that improved renal function after arrest is predictive of
443 long-term outcomes (7,8). It is not clear, however, whether or not early cardiac outcomes are predictive
444 of survival (6,69). Our analysis was not powered to look for survival benefit in human subjects, but such
445 a study is warranted.

446 In summary, we provide evidence in both a mouse model and retrospective clinical study that
447 metformin pretreatment offers significant cardiac and renal protection acutely after SCA. Our SCA
448 mouse involves cardiac injury without cardiac cell death, making it a more relevant system in which to
449 study metformin's mechanism of action. Direct AMPK activation and inhibition studies confirmed that
450 AMPK activation is necessary and sufficient for the cardiac and renal benefits observed with metformin
451 treatment. A number of molecular mechanisms exist downstream of AMPK activation, and we have
452 implicated changes to autophagy and mitochondrial dynamics in our mouse studies, though there were
453 no dramatic changes to mitochondrial morphology or electron transport chain subunit expression.
454 Future studies are warranted to investigate specific pathways downstream of metformin and AMPK that
455 may be useful as an acute rescue therapy to replicate the cardiac and renal protection seen in our model
456 and patient studies.

457

458

Methods

Pre-clinical Data

Sudden Cardiac Arrest Model

Eight-week-old male and female C57BL/6J mice (Jackson Labs, Bar Harbor, ME, #000664) underwent cardiac arrest by delivery of potassium chloride (KCl) directly into the LV by percutaneous, ultrasound-guided needle injection as previously described (31). Briefly, mice were anesthetized using vaporized isoflurane (Henry Schein, Melville, NY, #1182097) and endotracheally intubated, then mechanically ventilated (MiniVent, Harvard Apparatus, Holliston, MA, #73-0043) at a rate of 150 bpm and volume of 125 µL for females and 140 µL for males. Body temperature was maintained by utilizing a rectal temperature probe and heating pad (Indus Instruments, Webster, TX, #THM150). The chest was cleaned of hair using Nair and sterilized with betadine prior to introduction of a 30-gauge needle into the LV under ultrasound guidance (Visual Sonics Vevo 3100 with Vevo LAB v 5.5.1 software, Toronto, Canada), followed by delivery of 40 µL of 0.5M KCl to induce asystole. The ventilator was discontinued, and mice remained in asystole for a total of 8 minutes. 7.5 minutes after KCl dosing, 500 µL of 15 µg/mL epinephrine in saline (37°C) was injected into the LV over approximately 30 seconds. At 8 minutes, CPR was initiated by finger compression at about 300 bpm for 1-minute intervals. Electrocardiogram (ECG) was evaluated for return of sinus rhythm after each 1-minute interval. Animals not achieving ROSC by 3 minutes after CPR initiation were euthanized. Mice remained on the ventilator until breathing frequency was greater than 60 times per minute. Sham mice received no KCl, but rather a single injection of epinephrine. All animals were placed in a recovery cage under a heat lamp after the procedure.

Animal Treatment Groups

Treatment groups in the study were as follows: untreated sham, untreated cardiac arrest, metformin-pretreated sham, metformin-pretreated cardiac arrest, 5-aminoimidazole-4-carboxamide-1-beta-D-ribofuranoside (AICAR) pretreated cardiac arrest, metformin + compound c pretreated cardiac arrest, metformin rescue treatment cardiac arrest, and low-dose metformin pretreatment cardiac arrest. Metformin pretreatment consisted of *ad libitum* access to metformin (Major Pharmaceuticals, Livonia, MI, #48152) in drinking water (1 mg/mL) for 14 days prior to surgery. AICAR pretreated mice were given IP injections of 500 mg/kg AICAR (Toronto Research Chemicals, Toronto, CA, #A611700) in saline every other day for 14 days prior to surgery. Compound C pretreated mice were given 20 mg/kg IP injections of compound C (Cayman Chemical, Ann Arbor, MI, #11967) in saline daily for 14 days prior to arrest. Metformin rescue therapy was given as a single direct LV injection (1250 µg/kg) dissolved in saline along with 500 µL of 1mg/mL epinephrine (Par Pharmaceutical, Chestnut Ridge, NY, #10977) at the time of resuscitation. Low-dose metformin pretreatment consisted of *ad libitum* access to metformin in drinking water (0.2 mg/mL) for 14 days prior to surgery.

Echocardiography and Ultrasound

Immediately prior to arrest surgery, mice were evaluated by transthoracic echocardiography using Vevo 3100 imaging systems (Visual Sonics) with a 40MHz probe. Repeat echocardiography was performed one day after arrest under isoflurane anesthesia delivered by nose cone. Heart rate was maintained between 400-500 bpm during imaging by adjusting isoflurane concentration. B-mode images taken from the parasternal long-axis were captured and LV EF calculated using modified Simpson's

methods (70). A cohort of all groups were assessed for renal perfusion after resuscitation. The ultrasound probe was oriented transversely across the abdomen at the plane of the right kidney and monitored for renal artery blood flow by doppler imaging. Image analysis was performed by a blinded sonographer (Vevo Lab 5.5.1, Visual Sonics).

Tissue and Serum Collection

After euthanasia with isoflurane and cervical dislocation, mice underwent cardiac puncture for collection of blood by heparinized syringe. Blood was separated by centrifugation at 2,000 x g at 4°C for 10 minutes and the serum was flash frozen. These samples were evaluated for blood urea nitrogen (BUN), creatinine, alanine aminotransferase (ALT), and creatine kinase (CK) by the Kansas State Veterinary Diagnostic Laboratories (Manhattan, KS). Hearts from the mice were excised and LVs were isolated and flash frozen.

Western Blot

Frozen LV tissue was homogenized in lysis buffer containing a protease/phosphatase cocktail (Sigma-Aldrich, St. Louis, MO, #11697498001) and normalized for protein content using a BCA assay (Life Technologies, Carlsbad, CA, #23235). Samples were separated on NuPage 4-12% gradient SDS-PAGE gels (ThermoFisher, Waltham, MA, #WG1403BOX) and transferred onto iBlot nitrocellulose membranes (Invitrogen, #IB301001). Membranes were blocked in 5% milk for 1 hour and then incubated overnight at 4°C with primary antibodies, including OxPhos Rodent Antibody Cocktail 1:5000 (ThermoFisher, #458099), p-AMPK (Thr172, 1:1000, Cell Signaling, Danvers, MA, #2535), AMPK (1:1000, Cell Signaling, #2532), p-mTOR (Ser2448, 1:1000, Cell Signaling, #2971), DRP1 (1:1000, Cell Signaling, #5391), pDRP1 (Ser616, 1:1000, Thermo, #PA5-64821), mTOR (1:1000, Cell Signaling, #2972), p-S6 (Ser240/244, 1:1000, Cell Signaling, #2215), S6 (1:1000, Cell Signaling, #2217), p-AKT (Ser473, 1:1000, Cell Signaling, #9271), AKT (1:1000, Cell Signaling, #9272), p62 (1:1000, Sigma-Aldrich, #P0067), and GAPDH (1:5000, Millipore, St. Louis, MO, #AB2302). Following incubation, membranes were washed with TBS-tween and then probed for 1 hour at room temperature with anti-mouse or anti-rabbit secondary antibodies (Jackson ImmunoResearch, West Grove, PA, #115-035-003 and #115-035-144). Images were obtained by developing on a ChemiDoc XRS imaging system (BioRad, Hercules, CA) and analyzed using ImageJ software (National Institutes of Health, Bethesda, MD).

Tissue Histology

Kidneys were fixed overnight in 10% formalin (Thermo, #SF100) at 4°C, then washed with PBS and transferred to 70% ethanol at room temperature. After fixation and dehydration, tissues were embedded in paraffin prior to sectioning at 4 µm by the Histology Core at the Children's Hospital of Pittsburgh. Sections were stained with hematoxylin and eosin (H&E). Renal tubular pathology was semi-quantitatively scored (0: no injury to 4: severe injury) in terms of tubular dilatation, formation of proteinaceous casts, and loss of brush border(71). Histological scoring was performed in a blinded fashion at 40x magnification on outer medullary regions of the tissue sections. Eight fields were evaluated per kidney (n=6-8 animals/group). Samples were imaged using a Leica DM 2500 microscope (Leica, Wetzlar, Germany) and analyzed with LAS X software (Leica).

Transmission Electron Microscopy

LV tissue was immersion fixed in 2.5% glutaraldehyde in 0.1M PBS overnight at 4°C. Fixed samples were washed 3x in PBS then post-fixed in aqueous 1% OsO_4, 1% $K_3Fe(CN)_6$ for 1 hour at room

temperature. Following 3 PBS washes, the pellet was dehydrated through a graded series of 30-100% ethanol, and then 100% propylene oxide then infiltrated in 1:1 mixture of propylene oxide:Polybed 812 epoxy resin (Polysciences, Warrington, PA) for 1 hour. After several changes of 100% resin over 24 hours, the samples were embedded in molds and cured at 37°C overnight, followed by additional hardening at 65°C for two more days. Semi-thin (300 nm) sections were heated onto glass slides, stained with 1% toluidine blue and imaged using light microscopy to assure proper tissue orientation. Ultrathin (60-70 nm) sections were collected on 100 mesh copper grids, and stained with 4% uranyl acetate for 10 minutes, followed by 1% lead citrate for 7 min. Sections were imaged using a JEOL JEM 1400 PLUS transmission electron microscope (Peabody, MA) at 80 kV fitted with a side mount AMT digital camera (Advanced Microscopy Techniques, Danvers, MA). Twenty random images were obtained from sections throughout each LV. Individual mitochondria (n=50/sample) were randomly selected and traced for blinded quantification of size, roundness, and density via ImageJ (v1.8.0) software(72).

RNA Isolation, qPCR, and Microarray Analysis

Total genomic and mitochondrial DNA were isolated from frozen, powdered LV tissue. Tissue was homogenized in a buffer containing Proteinase K digestion buffer and proteinase K (Genesee Scientific, Genesee, NY, #42-700) overnight at 55°C, as previously described (73,74). The next day, DNA was purified by centrifuging the homogenized buffer with staged EtOH resuspension, followed by centrifugation and resuspension in TE buffer supplemented with RNase A (Invitrogen, #12091039). DNA concentration was measured using an AccuBlue Broad Range kit (Biotium, Fremont, CA, #31009). Relative mtDNA abundance was measured using a TaqMan primer/probe for mitochondrial ND1 (VIC-labeled; primer:probe 1:1) versus nuclear HDAC1 (FAM-labeled; primer:probe of 3:1; supplemental Table 1). Multiplex assessment of relative abundance of mtDNA was quantified using real-time quantitative PCR (qPCR) with TaqMan Fast Advanced Master Mix (ThermoFisher, #4444965) performed on QuantStudio 5 PCR system (Applied Biosystems). 4.6 ng of DNA was included in each reaction with 5 µM of primers/probes in a 10 µL total reaction volume and calculated by the ΔΔCq method (75). The qPCR amplification profile was: one cycle (95°C for 20 seconds) followed by 40 cycles (95°C for 1 sec then 60°C for 20 seconds). All primers and probes were produced by Integrated DNA Technologies (Coralville, Iowa).

mtDNA damage was assessed by comparing total PCR product after long-amplicon mtDNA replication with LongAmp Hot Start Taq Polymerase (New England Biolabs, Ipswich PA, #M0533; Supplemental Table 1)(76). 15 ng of DNA was amplified using the following profile: one cycle (94°C for 2 minutes) followed by 17 cycles (94°C for 15 seconds then 64°C for 12 seconds) then 1 cycle (72°C for 10 min)(77). Final product was measured by Accublue within the linear detection range. Specific DNA products were confirmed by gel electrophoresis.

Microarray analysis was performed on cDNA through the Affymetrix microarray analysis service (ThermoFisher). Eight untreated sham and eight untreated arrest mice were included in these studies with an even distribution of males and females. Differential gene expression analysis was performed using Transcription Analysis Console (Thermofisher). Gene-level p-values less than 0.05 were considered significant for gene inclusion. Subsequent pathway analysis was performed to compare untreated sham and arrest groups through Ingenuity Pathway Analysis (Qiagen). Complete datasets were deposited in GEO (accession no. GSE176494).

Statistical Analysis

Data were expressed as mean ± standard error in all figures. $p \leq 0.05$ was considered significant for all comparisons. One-way ANOVA with either Dunnett's multiple comparisons test or Tukey's multiple comparisons post-hoc analysis was used to compare groups either to a single group or all groups as detailed in figure legends. All statistical analysis was completed using Graphpad Prism 8 software (San Diego, CA).

Clinical Data

Clinical Data Collection

De-identified adult patients with a documented history of diabetes mellitus treated at a single academic medical center after resuscitation from cardiac arrest from January 2010 to December 2019 were included in this study. Patients with a history of known kidney disease prior to arrest, patients who arrived at our facility over 24 hours after collapse, patients for whom home medications were unknown, patients who rearrested and died before blood work could be acquired, and patients resuscitated with extracorporeal support were excluded from analysis. Demographic and arrest characteristics from a prospective registry, including patient age, sex, shockable presenting arrest rhythm, witnessed arrest, layperson CPR, arrest duration, number of epinephrine doses administered, cardiac etiology of arrest, and Charlson Comorbidity Index were extracted. Admission pharmacy documentation in each patient's electronic medical record was evaluated to determine whether patients were prescribed metformin, insulin, or other oral antihyperglycemic medications prior to their arrest, and classified each of these as three independent binary predictors. The primary outcomes of interest were peak serum creatinine and peak serum troponin at 24 hours post-arrest.

Clinical Statistical Analysis

Baseline population characteristics and outcomes were summarized using descriptive statistics. Multiple imputation with chained equations with predictive mean matching was used to impute missing continuous variables. Generalized linear models with a gamma distribution and log link were used to test the association of metformin with peak 24-hour serum creatinine and peak 24-hour serum troponin. For primary adjusted analysis, covariates were included based on biological plausibility. A series of sensitivity analyses, including a backward stepwise model sequentially removing predictors with $p<0.1$, complete case analysis, and adjusted modeling were performed, excluding patients receiving insulin who may be fundamentally sicker than those receiving no medications or oral antihyperglycemics only.

Study Approvals

All mouse studies were performed at the University of Pittsburgh in compliance with the National Institutes of Health Guidance for Care and Use of Experimental Animals. This protocol was approved by the University of Pittsburgh Animal Care and Use Committee (Protocol #18032212). The University of Pittsburgh Human Research Protection Office approved all aspects of the reported human subject's research with a waiver of informed consent due to its no greater than minimal risk to participants (STUDY19020205).

Author Contributions

CR, CD, and BK were responsible for conceptualization of these studies. CR designed the methodology and with CL and KR performed the investigation. CR and JE were responsible for data curation. Formal analyses were performed by CR, CL, TC, SSL, CD, and JE. Visualization was completed by TC and DS. CR, SSL, CD, JE, and BK wrote the manuscript. SSL and BK supervised the project, and BK provided resources for its completion. All authors reviewed the final manuscript and are responsible for its integrity.

Acknowledgements

Research reported in this manuscript was supported by: American Heart Association Transformational Project Award 18TPA34230048, NIH Instrument Grant for Advanced High-Resolution Rodent Ultrasound Imaging System 1S10OD023684-01A1, NIH Training Program in Imaging Sciences in Translational Cardiovascular Research 5T32HL129964-02, NIH 5K23NS097629 (to JE), and Richard K. Mellon Institute Award for postdoctoral trainees (to TC). Graphical abstract created with BioRender.com.

References

1. Aparicio HJ, Benjamin EJ, Callaway CW, et al. *Heart Disease and Stroke Statistics-2021 Update A Report from the American Heart Association*.; 2021. doi:10.1161/CIR.0000000000000950

2. Zipes D, Wellens HJJ. Sudden Cardiac Death. *Clin Cardiol*. Published online 1998:2334-2351.

3. Mongardon N, Dumas F, Ricome S, et al. Postcardiac arrest syndrome: from immediate resuscitation to long-term outcome. *Ann Intensive Care*. 2011;1(45):1-11.

4. Neumar RW, Nolan JP, Adrie C, et al. Post-cardiac arrest syndrome: Epidemiology, pathophysiology, treatment, and prognostication a consensus statement from the International Liaison Committee on Resuscitation. *Circulation*. 2008;118(23):2452-2483. doi:10.1161/CIRCULATIONAHA.108.190652

5. Ruiz-Bailén M, Aguayo De Hoyos E, Ruiz-Navarro S, et al. Reversible myocardial dysfunction after cardiopulmonary resuscitation. *Resuscitation*. 2005;66(2):175-181. doi:10.1016/j.resuscitation.2005.01.012

6. Chang WT, Ma MHM, Chien KL, et al. Postresuscitation myocardial dysfunction: Correlated factors and prognostic implications. *Intensive Care Med*. 2007;33(1):88-95. doi:10.1007/s00134-006-0442-9

7. Park YS, Choi YH, Oh JH, et al. Recovery from acute kidney injury as a potent predictor of survival and good neurological outcome at discharge after out-of-hospital cardiac arrest. *Crit Care*. 2019;23(1):1-11. doi:10.1186/s13054-019-2535-1

8. Storm C, Krannich A, Schachtner T, et al. Impact of acute kidney injury on neurological outcome and long-term survival after cardiac arrest – A 10□year observational follow up. *J Crit Care*. 2018;47:254-259. doi:10.1016/j.jcrc.2018.07.023

9. Maruthur NM, Tseng E, Hutfless S, Wilson LM, Suarez-cuervo C. Diabetes Medications as Monotherapy or Metformin-Based Combination Therapy for Type 2 Diabetes. *Ann Intern Med*. 2016;164:740-751. doi:10.7326/M15-2650

10. Han Y, Xie H, Liu Y, Gao P, Yang X, Shen Z. Effect of metformin on all□cause and cardiovascular mortality in patients with coronary artery diseases: a systematic review and an updated meta□analysis. *Cardiovasc Diabetol*. 2019;18(96):1-16. doi:10.1186/s12933-019-0900-7

11. Stumvoll M, Nurjhan N, Perriello G, Dailey G, Gerich JE. Metabolic Effects of Metformin in Non-Insulin-Dependent Diabetes Mellitus. *N Engl J Med*. 1995;333(9):550-554. doi:10.1056/nejm199508313330903

12. Wiernsperger NF, Bailey CJ. The Antihyperglycaemic Effect of Metformin. *Drugs*. 1999;58:31-39. doi:10.2165/00003495-199958001-00009

13. Zhou G, Goodyear LJ, Moller DE, et al. Role of AMP-activated protein kinase in mechanism of metformin action Find the latest version□: Role of AMP-activated protein kinase in mechanism of metformin action. *J Clin Invest*. 2001;108(8):1167-1174. doi:10.1172/JCI200113505.Introduction

14. Crowley MJ, Diamantidis CJ, Mcduffie JR, et al. Clinical Outcomes of Metformin Use in Populations With Chronic Kidney Disease , Congestive Heart Failure, or Chronic Liver Disease. *Ann Intern Med*. 2017;166:191-200. doi:10.7326/M16-1901

15. Bell S, Farran B, Mcgurnaghan S, et al. Risk of acute kidney injury and survival in patients treated with Metformin: an observational cohort study. *BMC Nephrol*. 2017;18(163):1-8. doi:10.1186/s12882-017-0579-5

16. Hassan FI, Sc M, Didari T, et al. A Review on The Protective Effects of Metformin in Sepsis-Induced Organ Failure. 2020;21(4). doi:10.22074/cellj.2020.6286.Introduction

17. Jochmans S, Alphonsine JE, Chelly J, et al. Does metformin exposure before ICU stay have any impact on patients' outcome? A retrospective cohort study of diabetic patients. *Ann Intensive Care*. 2017;7(116):1-9. doi:10.1186/s13613-017-0336-8

18. Reitz K, Marroquin O, Zenati M, et al. Association Between Preoperative Metformin Exposure and Postoperative Outcomes in Adults With Type 2 Diabetes. *JAMA Surg*. 2020;155(6). doi:10.1001/jamasurg.2020.0416.Association

19. Cameron AR, Morrison VL, Levin D, et al. Anti-Inflammatory Effects of Metformin Irrespective of Diabetes Status. *Circ Res*. 2016;119:652-665. doi:10.1161/CIRCRESAHA.116.308445

20. Chen Q, Lesnefsky EJ. Metformin and myocardial ischemia and reperfusion injury: Moving toward "prime time" human use? *Transl Res*. 2020;229:1-4. doi:10.1016/j.trsl.2020.10.006

21. Higgins L, Palee S, Chattipakorn SC, Chattipakorn N. Effects of metformin on the heart with ischaemia-reperfusion injury: Evidence of its benefits from in vitro, in vivo and clinical reports. *Eur J Pharmacol*. 2019;858(April):172489. doi:10.1016/j.ejphar.2019.172489

22. Kim TT, Dyck JRB. Is AMPK the savior of the failing heart? *Trends Endocrinol Metab*. 2015;26(1):40-48. doi:10.1016/j.tem.2014.11.001

23. Cao Y, Bojjireddy N, Kim M, et al. Activation of γ2-AMPK suppresses ribosome biogenesis and protects against myocardial ischemia/reperfusion injury. *Circ Res*. 2017;121(10):1182-1191. doi:10.1161/CIRCRESAHA.117.311159

24. Zaha V, Qi D, Su K, et al. AMPK Is Critical for Mitochondrial Function during Reperfusion. *J Mol Cell Cardiol*. 2017;21(2):129-139. doi:10.1016/j.yjmcc.2015.12.032.AMPK

25. Sullivan J, Brocklehurst K, Marley A, Carey F, Carling D, Beri R. Inhibition of lipolysis and lipogenesis in isolated rat adipocytes with AICAR, a cell-permeable activator of AMP-activated protein kinase. *FEBS Lett*. 1994;353:33-36.

26. Liu X, Chhipa RR, Nakano I, Dasgupta B. The AMPK inhibitor compound C is a potent AMPK-independent antiglioma agent. *Mol Cancer Ther*. 2014;13(3):596-605. doi:10.1158/1535-7163.MCT-13-0579

27. Dyck JRB, Lopaschuk GD. AMPK alterations in cardiac physiology and pathology: enemy or ally? *J Physiol*. 2006;1:95-112. doi:10.1113/jphysiol.2006.109389

28. Paiva MA, Gonçalves LM, Providência LA, Davidson SM, Yellon DM, Mocanu MM. Transitory activation of AMPK at reperfusion protects the ischaemic-reperfused rat myocardium against infarction. *Cardiovasc Drugs Ther*. 2010;24(1):25-32. doi:10.1007/s10557-010-6222-3

29. Paiva MA, Rutter-Locher Z, Gonçalves LM, et al. Enhancing AMPK activation during ischemia protects the diabetic heart against reperfusion injury. *Am J Physiol - Hear Circ Physiol*. 2011;300(6):2123-2134. doi:10.1152/ajpheart.00707.2010

30. Cates C, Rousselle T, Wang J, et al. Activated protein C protects against pressure overload-induced hypertrophy through AMPK signaling. *Biochem Biophys Res Commun*. 2018;495(4):1-18. doi:10.1016/j.bbrc.2017.12.125.Activated

31. Rutledge CA, Chiba T, Redding K, et al. A novel ultrasound-guided mouse model of sudden cardiac arrest. *PLoS One*. 2020;15(12):1-14. doi:10.1371/journal.pone.0237292

32. Lalau JD, Kajbaf F, Bennis Y, Hurtel-Lemaire AS, Belpaire F, De Broe ME. Metformin Treatment in Patients With Type 2 Diabetes and Chronic Kidney Disease Stages 3A, 3B, or 4. *Diabetes Care*. 2018;41(3):547-553. doi:10.2337/dc17-2231

33. Lalau JD, Arnouts P, Sharif A, De Broe ME. Metformin and other antidiabetic agents in renal failure patients. *Kidney Int*. 2015;87(2):308-322. doi:10.1038/ki.2014.19

34. Mohsin AA, Chen Q, Quan N, et al. Mitochondrial complex I inhibition by metformin limits reperfusion injury. *J Pharmacol Exp Ther*. 2019;369(2):282-290. doi:10.1124/jpet.118.254300

35. Stein SC, Woods A, Jones NA, Davison MD, Cabling D. The regulation of AMP-activated protein kinase by phosphorylation. *Biochem J*. 2000;345(3):437-443. doi:10.1042/0264-6021:3450437

36. Corton JM, Gillespie JG, Hawley SA, Hardie DG. 5-Aminoimidazole-4-Carboxamide Ribonucleoside: A Specific Method for Activating AMP-Activated Protein Kinase in Intact Cells? *Eur J Biochem*. 1995;229(2):558-565. doi:10.1111/j.1432-1033.1995.tb20498.x

37. Karamanlidis G, Nascimben L, Couper GS, Shekar PS, Del Monte F, Tian R. Defective DNA replication impairs mitochondrial biogenesis in human failing hearts. *Circ Res*. 2010;106(9):1541-1548. doi:10.1161/CIRCRESAHA.109.212753

38. Ge Y, Shi X, Boopathy S, McDonald J, Smith AW, Chao LH. Two forms of Opa1 cooperate to complete fusion of the mitochondrial inner-membrane. *Elife*. 2020;9:1-22. doi:10.1101/739078

39. Marsboom G, Toth PT, Ryan JJ, et al. Dynamin-related protein 1-mediated mitochondrial mitotic fission permits hyperproliferation of vascular smooth muscle cells and offers a novel therapeutic target in pulmonary hypertension. *Circ Res*. 2012;110(11):1484-1497. doi:10.1161/CIRCRESAHA.111.263848

40. Xiong W, Ma Z, An D, et al. Mitofusin 2 participates in mitophagy and mitochondrial fusion against angiotensin II-induced cardiomyocyte injury. *Front Physiol*. 2019;10(APR):1-12. doi:10.3389/fphys.2019.00411

41. Benischke AS, Vasanth S, Miyai T, et al. Activation of mitophagy leads to decline in Mfn2 and loss of mitochondrial mass in Fuchs endothelial corneal dystrophy. *Sci Rep*. 2017;7(1):1-11. doi:10.1038/s41598-017-06523-2

42. Kanamori H, Naruse G, Yoshida A, et al. Metformin Enhances Autophagy and Provides Cardioprotection in δ-Sarcoglycan Deficiency-Induced Dilated Cardiomyopathy. *Circ Hear Fail*. 2019;12(4):1-13. doi:10.1161/CIRCHEARTFAILURE.118.005418

43. Xie Z, Lau K, Eby B, et al. Improvement of cardiac functions by chronic metformin treatment is associated with enhanced cardiac autophagy in diabetic OVE26 mice. *Diabetes*. 2011;60(6):1770-1778. doi:10.2337/db10-0351

44. Sciarretta S, Maejima Y, Zablocki D, Sadoshima J. The Role of Autophagy in the Heart. *Annu Rev*

Physiol. 2018;80:1-26. doi:10.1146/annurev-physiol-021317-121427

45. Wu X, He L, Cai Y, et al. Induction of autophagy contributes to the myocardial protection of valsartan against ischemia-reperfusion injury. *Mol Med Rep*. 2013;8(6):1824-1830. doi:10.3892/mmr.2013.1708

46. Seibenhener ML, Babu JR, Geetha T, Wong HC, Krishna NR, Wooten MW. Sequestosome 1/p62 Is a Polyubiquitin Chain Binding Protein Involved in Ubiquitin Proteasome Degradation. *Mol Cell Biol*. 2004;24(18):8055-8068. doi:10.1128/mcb.24.18.8055-8068.2004

47. Li L, Xu J, He L, et al. The role of autophagy in cardiac hypertrophy. *Acta Biochim Biophys Sin (Shanghai)*. 2016;48(6):491-500. doi:10.1093/abbs/gmw025

48. Mizushima N, Yoshimori T. How to interpret LC3 immunoblotting. *Autophagy*. 2007;3(6):542-545. doi:10.4161/auto.4600

49. Emelyanova L, Bai X, Yan Y, et al. Biphasic effect of metformin on human cardiac energetics. *Transl Res*. Published online 2020. doi:10.1016/j.trsl.2020.10.002

50. Zhou G, Myers R, Li Y, et al. Role of AMP-activated protein kinase in mechanism of metformin action. *J Clin Invest*. 2001;108(8):1167-1174. doi:10.1172/JCI13505

51. Lesnefsky EJ, Chen Q, Hoppel CL. Mitochondrial Metabolism in Aging Heart. *Circ Res*. 2016;118(10):1593-1611. doi:10.1161/CIRCRESAHA.116.307505

52. Wang X, Yang L, Kang L, et al. Metformin attenuates myocardial Ischemia-reperfusion injury via Up-regulation of antioxidant enzymes. *PLoS One*. 2017;12(8):1-13. doi:10.1371/journal.pone.0182777

53. Whittington HJ, Hall AR, McLaughlin CP, Hausenloy DJ, Yellon DM, Mocanu MM. Chronic metformin associated cardioprotection against infarction: Not just a glucose lowering phenomenon. *Cardiovasc Drugs Ther*. 2013;27(1):5-16. doi:10.1007/s10557-012-6425-x

54. Solskov L, Løfgren B, Kristiansen SB, et al. Metformin induces cardioprotection against ischaemia/reperfusion injury in the rat heart 24 hours after administration. *Basic Clin Pharmacol Toxicol*. 2008;103(1):82-87. doi:10.1111/j.1742-7843.2008.00234.x

55. Gundewar S, Calvert, John W, Jha S, et al. Activation of AMPK by Metformin Improves Left Ventricular Function and Survival in Heart Failure. *Circ Res*. 2009;454(1):42-54. doi:10.1161/CIRCRESAHA.108.190918.Activation

56. Calvert JW, Gundewar S, Jha S, et al. Acute metformin therapy confers cardioprotection against myocardial infarction via AMPK-eNOS- mediated signaling. *Diabetes*. 2008;57(3):696-705. doi:10.2337/db07-1098

57. Bhamra GS, Hausenloy DJ, Davidson SM, et al. Metformin protects the ischemic heart by the Akt-mediated inhibition of mitochondrial permeability transition pore opening. *Basic Res Cardiol*. 2008;103(3):274-284. doi:10.1007/s00395-007-0691-y

58. Wang M, Weng X, Guo J, Chen Z, Jiang G, Liu X. Metformin alleviated EMT and fibrosis after renal ischemia-reperfusion injury in rats. *Ren Fail*. 2016;38(4):614-621. doi:10.3109/0886022X.2016.1149770

59. Corremans R, Vervaet BA, D'haese PC, Neven E, Verhulst A. Metformin: A candidate drug for

796 renal diseases. *Int J Mol Sci*. 2019;20(1):1-15. doi:10.3390/ijms20010042

797 60. Li J, Gui Y, Ren J, et al. Metformin protects against cisplatin-induced tubular cell apoptosis and
798 acute kidney injury via AMPKα-regulated autophagy induction. *Sci Rep*. 2016;6(April):1-11.
799 doi:10.1038/srep23975

800 61. Cao J, Meng S, Chang E, et al. Low concentrations of metformin suppress glucose production in
801 hepatocytes through AMP-activated protein kinase (AMPK). *J Biol Chem*. 2014;289(30):20435-
802 20446. doi:10.1074/jbc.M114.567271

803 62. Wang Y, An H, Liu T, et al. Metformin Improves Mitochondrial Respiratory Activity through
804 Activation of AMPK. *Cell Rep*. 2019;29(6):1511-1523.e5. doi:10.1016/j.celrep.2019.09.070

805 63. Lesnefsky EJ, Chen Q, Tandler B, Hoppel CL. Mitochondrial Dysfunction and Myocardial Ischemia-
806 Reperfusion: Implications for Novel Therapies. *Annu Rev Pharmacol Toxicol*. 2017;57:535-565.
807 doi:10.1146/annurev-pharmtox-010715-103335

808 64. Moussa A, Li J. AMPK in myocardial infarction and diabetes: the yin/yang effect. *Acta Pharm Sin*
809 *B*. 2012;2(4):368-378. doi:10.1016/j.apsb.2012.06.001

810 65. Takagi H, Matsui Y, Hirotani S, Sakoda H, Asano T, Sadoshima J. AMPK mediates autophagy during
811 myocardial ischemia in vivo. *Autophagy*. 2007;3(4):405-407. doi:10.4161/auto.4281

812 66. Toyama E, Herzig S, Courchet J, et al. AMP-activated protein kinase mediates mitochondrial
813 fission in response to energy stress. *Sci Rep*. 2016;351(6270):275-282.

814 67. Wang Q, Wu S, Zhu H, et al. Deletion of PRKAA triggers mitochondrial fission by inhibiting the
815 autophagy-dependent degradation of DNM1L. *Autophagy*. 2017;13(2):404-422.
816 doi:10.1080/15548627.2016.1263776

817 68. Vásquez-Trincado C, García-Carvajal I, Pennanen C, et al. Mitochondrial dynamics, mitophagy and
818 cardiovascular disease. *J Physiol*. 2016;594(3):509-525. doi:10.1113/JP271301

819 69. Jentzer JC, Chonde MD, Dezfulian C. Myocardial Dysfunction and Shock after Cardiac Arrest.
820 *Biomed Res Int*. 2015;2015:1-14.

821 70. Lang RM, Bierig M, Devereux RB, et al. Recommendations for chamber quantification: A report
822 from the American Society of Echocardiography's guidelines and standards committee and the
823 Chamber Quantification Writing Group, developed in conjunction with the European Association
824 of Echocardiograph. *J Am Soc Echocardiogr*. 2005;18(12):1440-1463.
825 doi:10.1016/j.echo.2005.10.005

826 71. Chiba T, Peasley KD, Cargill KR, et al. Sirtuin 5 regulates proximal tubule fatty acid oxidation to
827 protect against AKI. *J Am Soc Nephrol*. 2019;30(12):2384-2398. doi:10.1681/ASN.2019020163

828 72. Schneider CA, Rasband WS, Eliceiri KW. NIH Image to ImageJ: 25 years of image analysis. *Nat*
829 *Methods*. 2012;9(7):671-675. doi:10.1038/nmeth.2089

830 73. Kolesar JE, Wang CY, Taguchi Y V, Chou S, Kaufman BA. Two-dimensional intact mitochondrial
831 DNA agarose electrophoresis reveals the structural complexity of the mammalian mitochondrial
832 genome. 2013;41(4):1-14. doi:10.1093/nar/gks1324

833 74. Falabella M, Kolesar JE, Wallace C, et al. G-quadruplex dynamics contribute to regulation of
834 mitochondrial gene expression. *Sci Rep*. 2019;9(5605):1-17. doi:10.1038/s41598-019-41464-y

75. Livak KJ, Schmittgen TD. Analysis of relative gene expression data using real-time quantitative PCR and the 2-ΔΔCT method. *Methods*. 2001;25(4):402-408. doi:10.1006/meth.2001.1262

76. Gonzalez-Hunt CP, Rooney JP, Ryde IT, Anbalagan C, Joglekar R, Meyer JN. PCR-Based Analysis of Mitochondrial DNA Copy Number, Mitochondrial DNA Damage, and Nuclear DNA Damage. *Curr Protoc Toxicol*. 2016;67(1):20.11.1-20.11.25. doi:10.1002/0471140856.tx2011s67

77. Furda AM, Bess AS, Meyer JN, Van Houten B. Analysis of DNA damage and repair in nuclear and mitochondrial DNA of animal cells using quantitative PCR. *Methods Mol Biol*. 2012;920:111-132. doi:10.1007/978-1-61779-998-3-9

Figures and figure legends

Figure 1. Mouse model of sudden cardiac arrest (SCA) and Microarray Pathway Analysis. A) Cartoon representation of direct left ventricular injection of potassium chloride (KCl) to cause asystole with representative ultrasound image of needle guidance. B) Time course of SCA protocol. C) Pathway analysis of microarray data from left ventricles collected one day after SCA (n=8) versus sham (n=8) surgeries, demonstrating the ten most significantly changed canonical signaling pathways by Ingenuity Pathway Analysis (IPA). LV, left ventricle; ROSC, return of spontaneous circulation.

Figure 2. Metformin treated mice have preserved ejection fraction (EF) and lower kidney damage than untreated mice one day after sudden cardiac arrest (SCA). A) At baseline, there is no difference in EF between treatment groups. One day after SCA, EF in arrest mice (n=20) is significantly lower than sham mice (n=15). Metformin pretreatment did not change EF in mice receiving sham surgery (n=8), but metformin pretreatment did lead to higher EF at 24 hours post-SCA (n=20) when compared to untreated arrest mice. B) Representative histologic sections from untreated sham and untreated arrest mice demonstrating proteinaceous casts in renal tubules (black stars) and infiltrates (white arrowheads) with glomeruli marked (white X's). Scale bar = 50 μM. C) Markers of kidney damage, including serum creatinine, blood urea nitrogen (BUN), and histologic tubular injury score demonstrate significant injury in untreated arrest mice. Untreated sham (n=8) and metformin treated sham (n=6) mice have no evidence of damage. Metformin treated arrest mice (n=7) have significantly lower creatinine and tubular injury score than untreated arrest mice (n=8). D) There is no change in renal ischemic duration between untreated arrest and metformin treated arrest mice. E) Western blot analysis of pAMPK/AMPK in arrest mice pretreated with metformin when compared to sham, untreated arrest, and metformin-pretreated sham groups demonstrating increased p-AMPK/AMPK and p-AMPK/GAPDH (n=6 for all groups). Data are expressed as mean ± SEM. P-values: *< 0.05, **< 0.01, ***< 0.001 by one-way ANOVA with Tukey post-hoc analysis. EF, ejection fraction; BUN, blood urea nitrogen.

Figure 3. AMPK activation alone improves cardiac outcomes after SCA, and AMPK activation is necessary to exert metformin's cardioprotection. A) SCA mice pretreated with the AMPK-activator AICAR (Arrest AICAR; n=9) have improved EF when compared to untreated arrest mice (n=15; data presented in Figure 2). Mice pretreated with both metformin and the AMPK-inhibitor Compound C (Arrest Met + Comp C; n=9) have decreased EF when compared to untreated arrest mice. B) AICAR treatment causes significant p-AMPK/AMPK elevation when compared to untreated arrest mice (n=6 for all groups). Data are expressed as mean +/- SEM. P-values: *< 0.05, **< 0.01, ***< 0.001 by one-way ANOVA with Dunnett's post-hoc analysis (A) or Tukey post-hoc analysis (B). AICAR, 5-aminoimidazole-4-carboxamide-1-β-D-ribofuranoside; Comp C, Compound C; EF, ejection fraction.

Figure 4. Metformin affects mitochondrial characteristics after SCA. A) Representative electron microscope images of intrafibrillar mitochondria in untreated sham, untreated arrest, and metformin pretreated arrest mice one day after surgery (40,000x magnification). B) Mitochondria are smaller and

more circular in untreated arrest and metformin treated arrest mice when compared to sham, and metformin treated arrest mice have larger mitochondria than untreated arrest mice (n=50 per group). C) Electron transport chain expression is largely unchanged between treatment groups, with the exception of complex II (CII) expression in metformin-pretreated arrest mice being significantly higher than untreated sham mice one day after arrest (n=6/group, normalized to ponceau stain). D) mtDNA copy number is increased and has less damage in metformin treated arrest mice (n=7) when compared to untreated arrest mice (n=5). Untreated arrest mice had no changes to mtDNA copy number or damage when compared to sham. Data are expressed as mean ± SEM. P-values: *< 0.05, **< 0.01, ***< 0.001 by one-way ANOVA with Tukey post-hoc analysis. ND1, NADH dehydrogenase 1; HDAC1, Histone deacetylase 1; mtDNA, mitochondrial DNA; WT, wild-type.

Figure 5. Metformin pretreatment affects autophagy and mitochondrial dynamics after sudden cardiac arrest (SCA). A) Representative western blot images of markers of mitochondrial fission and fusion. Mitofusin 2 (MFN2) is significantly depressed in metformin treated arrest mice (n=6) compared to untreated sham (n=6), untreated arrest (n=6), and sham metformin (n=5) groups. OPA1 is significantly depressed in metformin treated arrest compared to untreated arrest mice. There is no significant change to p-DRP expression between groups. B) Representative western blot images of autophagy related proteins downstream of AMPK. p-mTOR expression is reduced in untreated arrest, metformin treated sham, and metformin treated arrest mice when compared to untreated sham, and metformin treated mice have lower total mTOR than untreated sham and arrest groups. p-S6, a marker of mTOR activity, is also reduced in untreated arrest and metformin treated arrest mice when compared to sham. S6 expression is increased in sham metformin mice, but depressed in metformin arrest mice compared to sham, while the p-S6/S6 ratio is only significantly changed in the untreated arrest mice when compared to sham. P62, a marker of autophagosome formation, is lower in metformin treated arrest mice compared to untreated arrest mice. Untreated arrest mice have significantly elevated LC3II/LC3I, a marker of autophagy, compared to sham mice and metformin treated arrest mice (n=6/group). Data are expressed as mean ± SEM. P-values: *< 0.05, **< 0.01, ***< 0.001 by one-way ANOVA with Tukey post-hoc analysis for all groups, except for the p-S6 analyses, which used Dunnett's post-hoc analysis. DRP, dynamin-related protein1; LC3, microtubule-associated protein light chain; MFN2, mitofusin 2; mTOR, mechanistic target of rapamycin; OPA1, dynamin-like 120 kDa protein, mitochondrial.

Figure 6. Metformin does not work as a rescue therapy following arrest. A) When given concomitantly with epinephrine, intravenous metformin (n=6) did not demonstrate any change to ejection fraction (EF) when compared to untreated arrest mice (n=15; data presented in Figure 2) or metformin treated arrest mice (n=20, data presented in Figure 2). P-values: *< 0.05 by one-way ANOVA with Tukey post-hoc analysis.

Figure 7. Summary of clinical inclusion and exclusion data for retrospective analysis of the Pittsburgh Post-Cardiac Arrest Service patient database. Primary outcomes evaluated included peak serum troponin and peak serum creatinine in diabetic patients with and without a history of metformin therapy.

926

927 **Figure 8. Distributions of peak 24-hour serum troponin and peak 24-hour serum creatinine for diabetic**
928 **patients with and without metformin therapy prior to arrest.** Dashed lines represent median values
929 and dotted lines represent upper and lower quartiles.

930

931

932

933 **Table Legends**

934

935 **Table 1. Surgical data for arrest mice.** There are no significant changes to body weight or body
936 temperature at time of extubation between treatment groups. There is no change in time to return of
937 spontaneous circulation (ROSC) or time to extubation between untreated arrest and treated arrest
938 groups. There is no change to random blood glucose 24-hours after arrest between sham, untreated
939 arrest, and metformin pretreated arrest mice. Data are presented as mean ± SEM unless otherwise
940 noted. Analysis by one-way ANOVA with Tukey post-hoc analysis.

941

942 **Table 2. Baseline demographics and clinical characteristics.** Data are presented as mean ± standard
943 deviation, median [interquartile range], or sample number (corresponding percentage).

944

945 **Table 3. Association between metformin use and peak serum creatine and troponin by log link model.**
946 Model was adjusted for age, sex, arrest location (in- vs out-of-hospital), witnessed collapse, layperson
947 cardiopulmonary resuscitation, presenting rhythm, arrest duration, number of epinephrine
948 administered, cardiac etiology of arrest, Charlson Comorbidity index, insulin, and other oral diabetic
949 medications. Both peak serum creatinine level and peak serum troponin level 24 hours post-arrest are
950 significantly associated with history of metformin use.

951

952

953

954

955

A

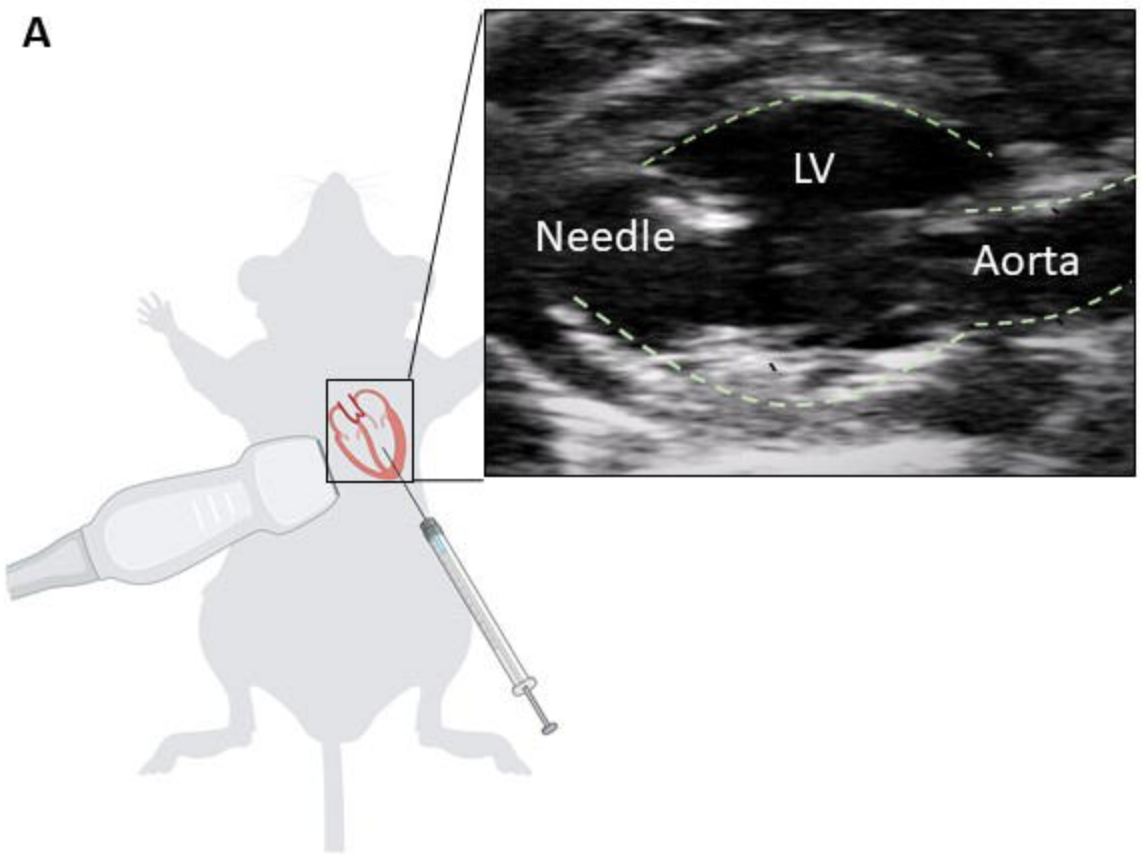

C

IPA Canonical Pathway	-log(p-val)	z-score
AMPK Signaling	5.38	2.121
NRF2-mediated Oxidative Stress	5.05	1.604
Xenobiotic Metabolism PXR Signaling	4.51	2.469
Hepatic Fibrosis	4.5	n/a
HIF1α Signaling	4.48	1.067
Autophagy	4.46	n/a
Insulin Receptor Signaling	3.97	1.3
Apelin Adipocyte Signaling Pathway	3.96	2.837
Unfolded Protein Response	3.9	0
TCA Cycle II (Eukaryotic)	3.76	2.53

B

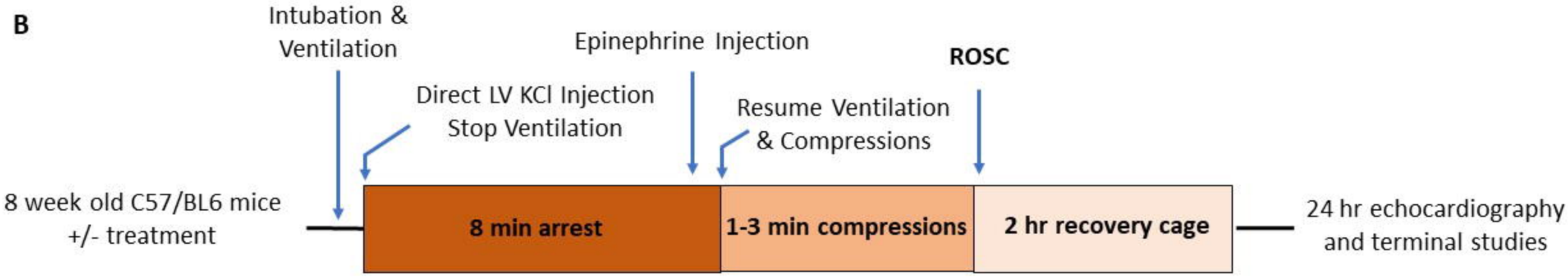

Figure 1. Mouse model of sudden cardiac arrest (SCA) and Microarray Pathway Analysis. A) Cartoon representation of direct left ventricular injection of potassium chloride (KCl) to cause asystole with representative ultrasound image of needle guidance. B) Time course of SCA protocol. C) Pathway analysis of microarray data from left ventricles collected one day after SCA (n=8) versus sham (n=8) surgeries, demonstrating the ten most significantly changed canonical signaling pathways by Ingenuity Pathway Analysis (IPA). LV, left ventricle; ROSC, return of spontaneous circulation.

Figure 2. Metformin treated mice have preserved ejection fraction (EF) and lower kidney damage than untreated mice one day after sudden cardiac arrest (SCA). A) At baseline, there is no difference in EF between treatment groups. One day after SCA, EF in arrest mice (n=20) is significantly lower than sham mice (n=15). Metformin pretreatment did not change EF in mice receiving sham surgery (n=8), but metformin pretreatment did lead to higher EF at 24 hours post-SCA (n=20) when compared to untreated arrest mice. B) Representative histologic sections from untreated sham and untreated arrest mice demonstrating proteinaceous casts in renal tubules (black stars) and infiltrates (white arrowheads) with glomeruli marked (white X's). Scale bar = 50 µM. C) Markers of kidney damage, including serum creatinine, blood urea nitrogen (BUN), and histologic tubular injury score demonstrate significant injury in untreated arrest mice. Untreated sham (n=8) and metformin treated sham (n=6) mice have no evidence of damage. Metformin treated arrest mice (n=7) have significantly lower creatinine and tubular injury score than untreated arrest mice (n=8). D) There is no change in renal ischemic duration between untreated arrest and metformin treated arrest mice. E) Western blot analysis of pAMPK/AMPK in arrest mice pretreated with metformin when compared to sham, untreated arrest, and metformin-pretreated sham groups demonstrating increased p-AMPK/AMPK and p-AMPK/GAPDH (n=6 for all groups). Data are expressed as mean ± SEM. P-values: *< 0.05, **< 0.01, ***< 0.001 by one-way ANOVA with Tukey post-hoc analysis. EF, ejection fraction; BUN, blood urea nitrogen.

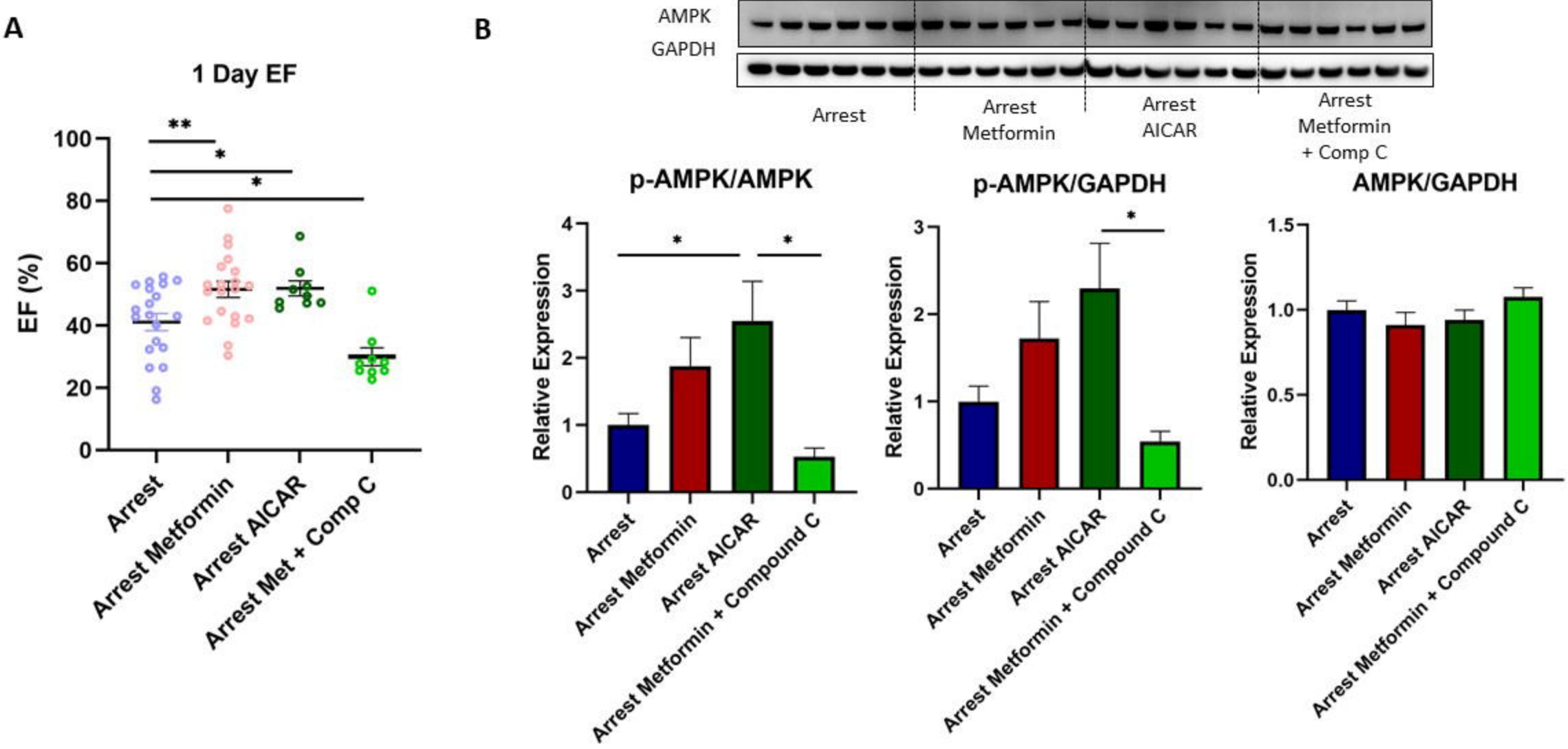

Figure 3. AMPK activation alone improves cardiac outcomes after SCA, and AMPK activation is necessary to exert metformin's cardioprotection. A) SCA mice pretreated with the AMPK-activator AICAR (Arrest AICAR; n=9) have improved EF when compared to untreated arrest mice (n=15; data presented in Figure 2). Mice pretreated with both metformin and the AMPK-inhibitor Compound C (Arrest Met + Comp C; n=9) have decreased EF when compared to untreated arrest mice. B) AICAR treatment causes significant p-AMPK/AMPK elevation when compared to untreated arrest mice (n=6 for all groups). Data are expressed as mean +/- SEM. P-values: *< 0.05, **< 0.01, ***< 0.001 by one-way ANOVA with Dunnett's post-hoc analysis (A) or Tukey post-hoc analysis (B). AICAR, 5-aminoimidazole-4-carboxamide-1-β-D-ribofuranoside; Comp C, Compound C; EF, ejection fraction.

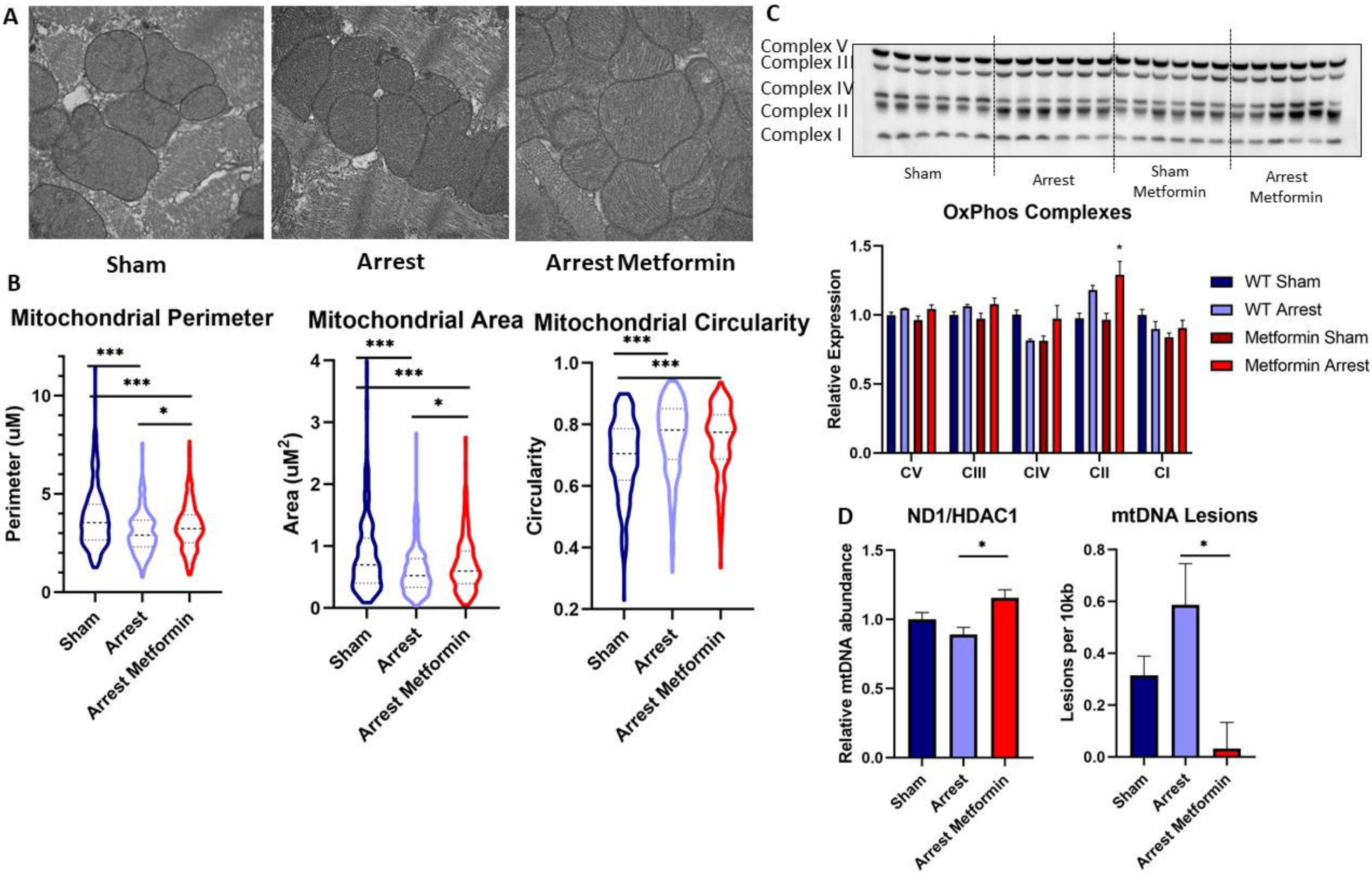

Figure 4. Metformin affects mitochondrial characteristics after SCA. A) Representative electron microscope images of intrafibrillar mitochondria in sham, untreated arrest and metformin pretreated arrest mice one day after surgery (40,000x magnification). B) Mitochondria are smaller and more circular in untreated arrest and metformin treated arrest mice when compared to sham, and metformin treated arrest mice have larger mitochondria than untreated arrest mice (n=50 per group). C) Electron transport chain expression is largely unchanged between treatment groups, with the exception of complex II (CII) expression in metformin-pretreated arrest mice being significantly higher than untreated sham mice one day after arrest (n=6/group, normalized to ponceau stain). D) mtDNA copy number is increased and has less damage in metformin treated arrest mice (n=7) when compared to untreated arrest mice (n=5). Untreated arrest mice had no changes to mtDNA copy number or damage when compared to sham. Data are expressed as mean ± SEM. P-values: *< 0.05, **< 0.01, ***< 0.001 by one-way ANOVA with Tukey post-hoc analysis. ND1, NADH dehydrogenase 1; HDAC1, Histone deacetylase 1; mtDNA, mitochondrial DNA; WT, wild-type.

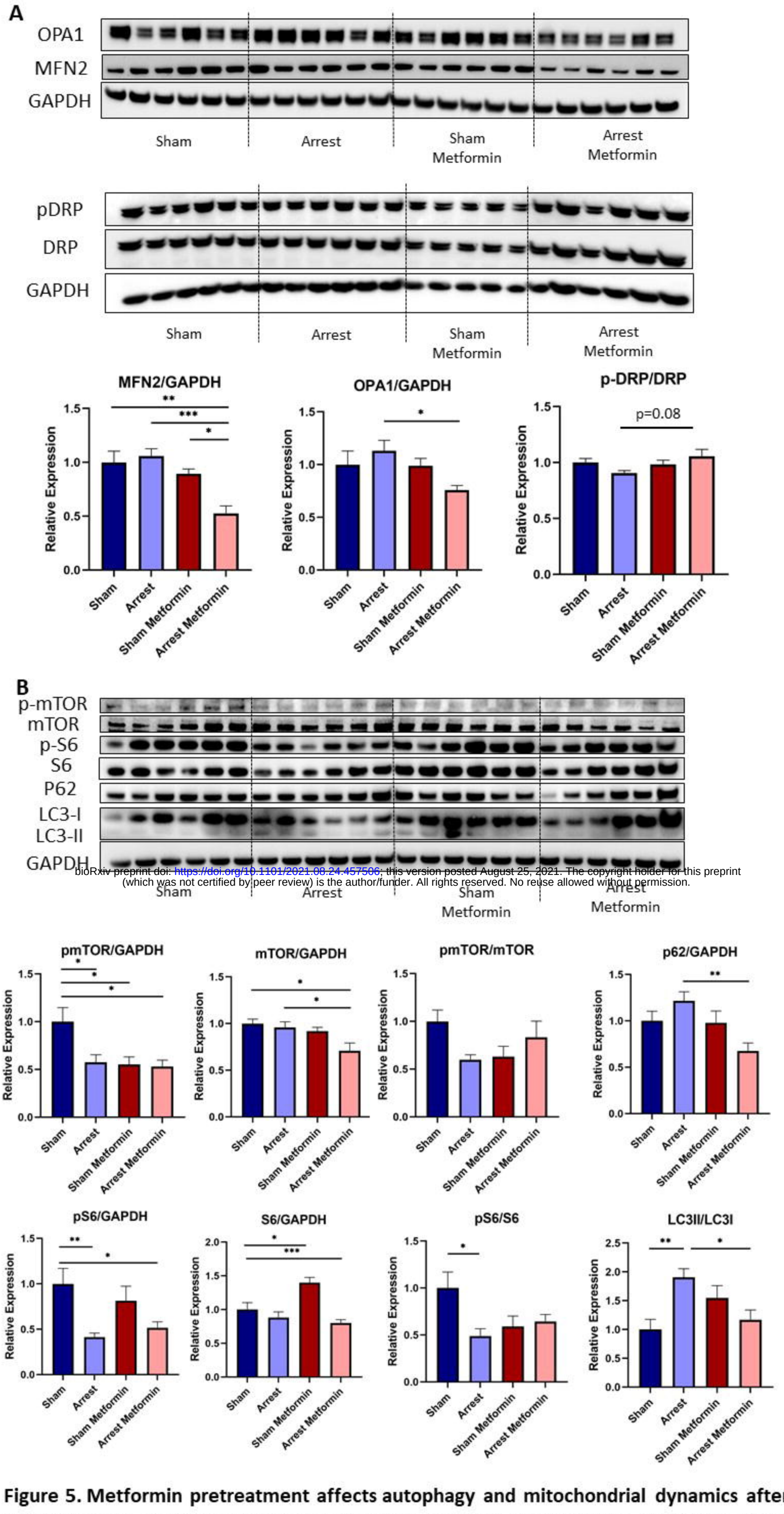

Figure 5. Metformin pretreatment affects autophagy and mitochondrial dynamics after sudden cardiac arrest (SCA). A) Representative western blot images of markers of mitochondrial fission and fusion. Mitofusin 2 (MFN2) is significantly depressed in metformin treated arrest mice (n=6) compared to untreated sham (n=6), untreated arrest (n=6), and sham metformin (n=5) groups. OPA1 is significantly depressed in metformin treated arrest compared to untreated arrest mice. There is no significant change to p-DRP expression between groups. B) Representative western blot images of autophagy related proteins downstream of AMPK. p-mTOR expression is reduced in untreated arrest, metformin treated sham, and metformin treated arrest mice when compared to untreated sham, and metformin treated mice have lower total mTOR than untreated sham and arrest groups. p-S6, a marker of mTOR activity, is also reduced in untreated arrest and metformin treated arrest mice when compared to sham. S6 expression is increased in sham metformin mice, but depressed in metformin arrest mice compared to sham, while the p-S6/S6 ratio is only significantly changed in the untreated arrest mice when compared to sham. P62, a marker of autophagosome formation, is lower in metformin treated arrest mice compared to untreated arrest mice. Untreated arrest mice have significantly elevated LC3II/LC3I, a marker of autophagy, compared to sham mice and metformin treated arrest mice (n=6/group). Data are expressed as mean ± SEM. P-values: *< 0.05, **< 0.01, ***< 0.001 by one-way ANOVA with Tukey post-hoc analysis for all groups, except for the p-S6 analyses, which used Dunnett's post-hoc analysis. DRP, dynamin-related protein1; LC3, microtubule-associated protein light chain; MFN2, mitofusin 2; mTOR, mechanistic target of rapamycin; OPA1, dynamin-like 120 kDa protein, mitochondrial.

A

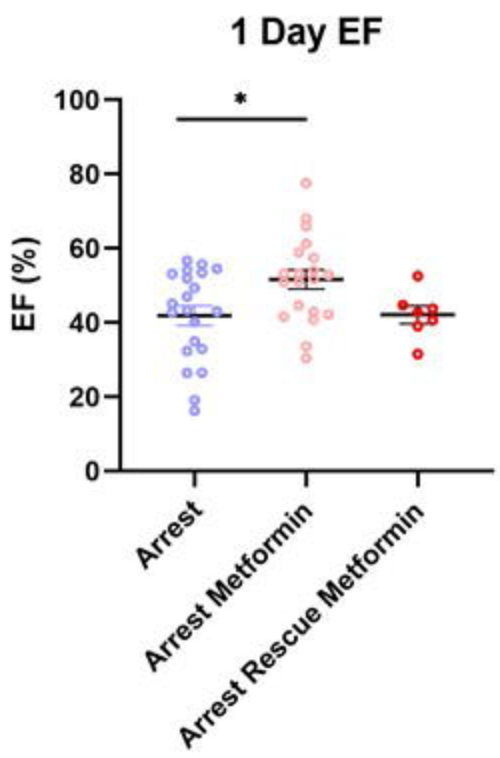

Figure 6. Metformin does not work as a rescue therapy following arrest. A) When given concomitantly with epinephrine, intravenous metformin (n=6) did not demonstrate any change to ejection fraction (EF) when compared to untreated arrest mice (n=15; data presented in Figure 2) or metformin treated arrest mice (n=20, data presented in Figure 2). P-values: *< 0.05 by one-way ANOVA with Tukey post-hoc analysis.

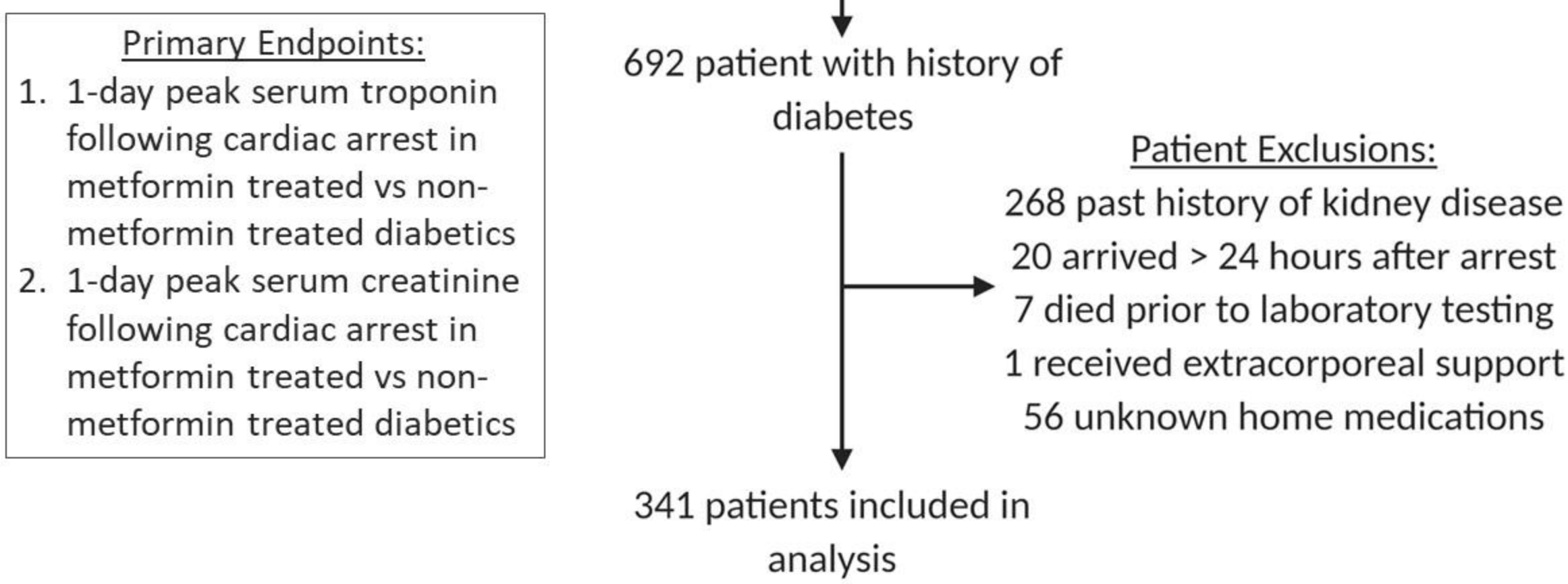

Figure 7. Summary of clinical inclusion and exclusion data for retrospective analysis of the Pittsburgh Post-Cardiac Arrest Service patient database. Primary outcomes evaluated included peak serum troponin and peak serum creatinine in diabetic patients with (n=122) and without (n=174) a history of metformin therapy.

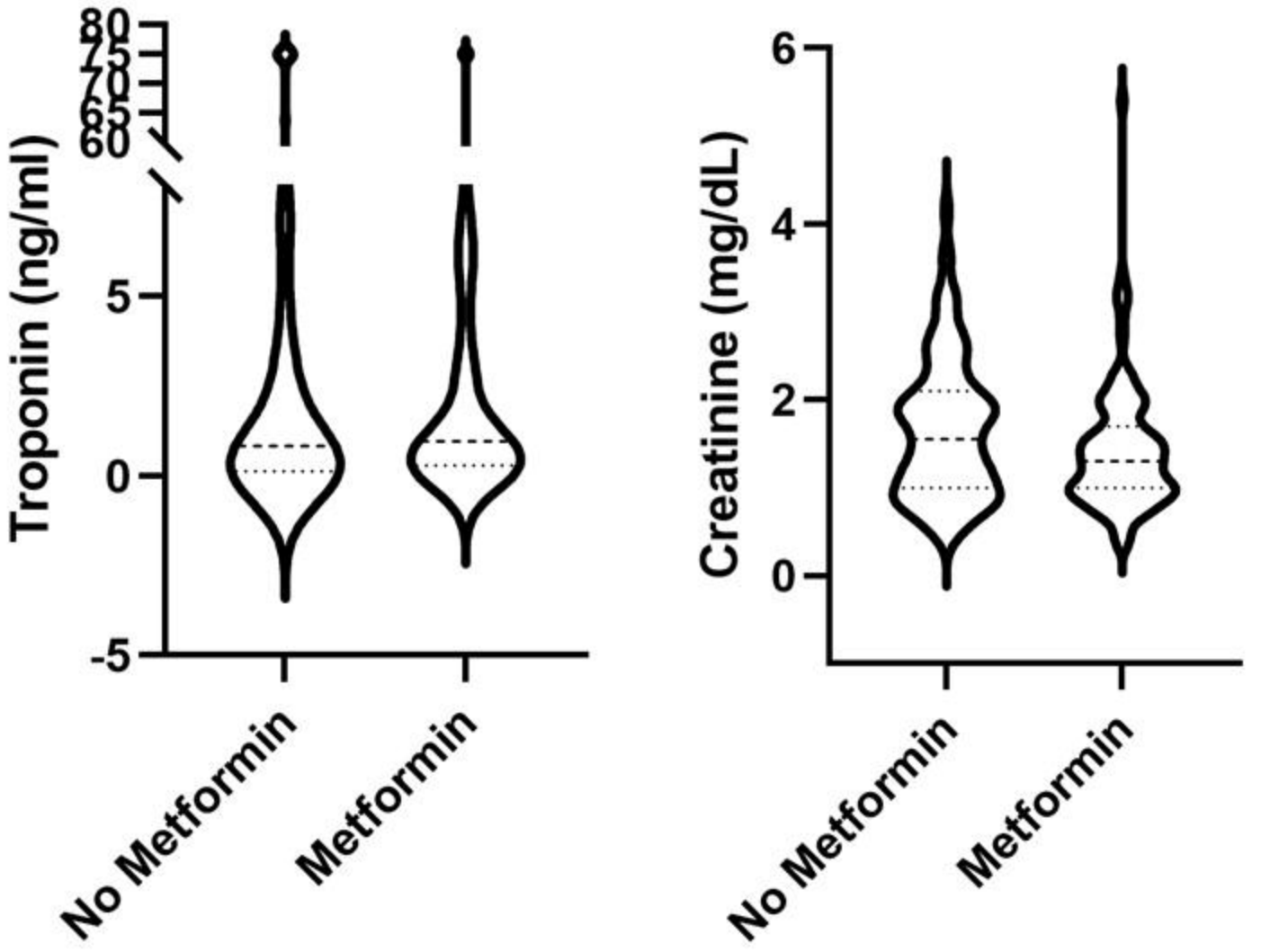

Figure 8. Distributions of peak 24-hour serum troponin and peak 24-hour serum creatinine for diabetic patients with and without metformin therapy prior to arrest. Dashed lines represent median values and dotted lines represent upper and lower quartiles.

Table 1. Surgical data for arrest mice. There are no significant changes to body weight or body temperature at time of extubation between treatment groups. There is no change in time to return of spontaneous circulation (ROSC) or time to extubation between untreated arrest and treated arrest groups. There is no change to random blood glucose 24-hours after arrest between sham, untreated arrest, and metformin pretreated arrest mice. Data are presented as mean ± SEM unless otherwise noted. Analysis by one-way ANOVA with Tukey post-hoc analysis.

	Sham (n=20)	Arrest (n=26)	Sham Metformin (n=8)	Arrest Metformin (n=21)	Arrest Low Dose Metformin (n=9)	Arrest AICAR (n=9)	Arrest Metformin+ Compound C (n=8)	Arrest Rescue Metformin (n=7)
Age (d)	57.55±0.68	57.60±0.59	58.75±0.40	58.80±0.48	60.33±0.53	58.44±0.50	58.75±0.37	60.71±0.61
# Female / Total Mice (percentage)	11/20 (55%)	12/26 (46%)	5/8 (63%)	12/21 (57%)	4/9 (44%)	4/9 (44%)	4/8 (50%)	3/7 (43%)
Body Wt (g)	23.19±0.83	22.97±0.62	21.05±0.88	21.77±0.78	20.86±0.84	22.59±1.1	22.47±1.23	22.46±1.34
Temp at Extubation (°C)	35.86±0.15	35.53±0.20	35.96±0.18	35.95±0.12	35.53±0.21	35.79±0.19	36.21±0.11	35.86±0.23
ROSC (min)	-	1.31±0.09	-	1.43±0.15	1.11±0.11	1.44±0.24	1.13±0.12	1.29±0.18
Time to Extubation (min)	-	22.31±0.66	-	23.64±0.32	22.72±0.49	22.06±0.90	24.06±0.52	22.71±0.84
Time to Kidney Reperfusion (min)	-	21.3±0.90	-	21.79±0.57	22.24±0.49	20.43±1.01	24.70±0.64	22.50±0.97
Random glucose 24 h after arrest (mmol/L)	184.3±25.0	205.8±10.0	-	218.8±28.0	-	-	-	-

Table 2. Baseline demographics and clinical characteristics. Data are presented as mean ± standard deviation, median [interquartile range], or sample number (corresponding percentage).

Characteristic	Overall cohort (n = 341)	Metformin (n = 140)	No metformin (n = 201)
Age, years	65 ± 13	65 ± 12	64 ± 14
Female sex	148 (43)	58 (41)	90 (45)
Arrest out-of-hospital	256 (75)	108 (77)	148 (74)
Shockable rhythm	109 (32)	39 (28)	70 (35)
Witnessed collapse	160 (47)	70 (50)	90 (45)
Layperson CPR	156 (46)	72 (51)	84 (42)
Epinephrine doses	2 [1 – 4]	3 [1 – 4]	2 [1 – 4]
Arrest duration, min	16 [8 – 27]	16 [8 – 32]	16 [8 – 23]
Cardiac etiology	96 (28)	36 (26)	60 (30)
Charlson Comorbidity index	2 [2 – 3]	2 [1 – 3]	3 [2 – 3]
Insulin	152 (45)	34 (24)	118 (59)
Other oral diabetic medication	92 (27)	47 (34)	45 (22)
Peak 24h troponin	0.88 [0.19 – 5.7]	0.97 [0.29 – 4.71]	0.84 [0.14 – 7.0]
Peak 24h creatinine	1.4 [1.0 – 2.0]	1.3 [1.0 – 1.7]	1.6 [1.0 – 2.1]

Table 3. Association between metformin use and peak serum creatine and troponin by log link model. Model was adjusted for age, sex, arrest location (in- vs out-of-hospital), witnessed collapse, layperson cardiopulmonary resuscitation, presenting rhythm, arrest duration, number of epinephrine administered, cardiac etiology of arrest, Charlson Comorbidity index, insulin, and other oral diabetic medications. Both peak serum creatinine level and peak serum troponin level 24 hours post-arrest are significantly associated with history of metformin use.

Endpoint	Coefficient (95% CI)	P value
Creatinine	-0.19 (-0.30 – -0.08)	0.001
Troponin	-1.29 (-2.11 – -0.46)	0.002